



Tectonics, Climate and Topography: Oxygen stable isotopes and the early Eocene growth of the Pyrenees

Louis Honegger¹, Thierry Adatte², Jorge E. Spangenberg³, Miquel Poyatos-Moré⁴, Alexandre Ortiz^{5,6},
 Magdalena Ellis Curry⁷, Damien Huyghe⁸, Cai Puigdefàbregas⁹, Miguel Garcés¹⁰, Andreu Vinyoles¹⁰,
 5 Luis Valero¹, Charlotte Läubli¹¹, Andrés Nowak¹, Andrea Fildani¹², Julian D. Clark¹³, Sébastien
 Castelltort^{1*}

¹Department of Earth Sciences, University of Geneva, Rue des Maraîchers 13, 1205 Geneva, Switzerland

²Institut of Earth Sciences, Géopolis, University of Lausanne, 1015 Lausanne, Switzerland

10 ³Institute of Earth Surface Dynamics (IDYST), Géopolis, University of Lausanne, 1015 Lausanne, Switzerland

⁴Department of Geosciences, University of Oslo, Sem Sælands vei 1, 0371 Oslo, Norway

⁵Université de Pau et des Pays de l'Adour, LFCR, UMR5150, 64000 Pau, France

⁶TOTAL, CSTJF, 64018, Pau Cedex, France

15 ⁷Department of Earth and Atmospheric Sciences 3507 Cullen Blvd. University of Houston

⁸INES ParisTech, PSL University, Centre de Géosciences, 35 rue St Honoré, 77305, Fontainebleau, Cedex, France

⁹Department of Earth and Ocean Dynamics, University of Barcelona, C/ Martí i Franquès, s/n, 08028 Barcelona, Spain

20 ¹⁰Department of Earth and Ocean Dynamics & Geomodels Research Institute, Faculty of Earth Sciences, Universitat de Barcelona, Spain

¹¹Freie Universität Berlin, Division of Tectonics and Sedimentary Geology, Malteserstr. 74-100, 12249 Berlin, Germany

¹²The Deep Time Institute, P.O. Box 27552, Austin, Texas 78755-7552, USA

25 ¹³Equinor Research Center, 6300 Bridge Point Parkway, Building 2, Suite 100, Austin, Texas, USA

Correspondence to: Sébastien Castelltort (sebastien.castelltort@unige.ch)

Abstract. The topographic history of an orogen, key element to study the interactions of the climate and tectonic conditions that drove it, can be reconstructed by inverting the sedimentary record of its adjacent basins. Previous tectono-stratigraphic studies, including flexural models, and sparse stable oxygen and carbon isotope data from the South-Pyrenean foreland basin suggest a major topographic rise occurred in the late Paleocene-early Eocene. To further test this hypothesis, we present a stack of 658 stable isotope measurements on whole-rock marine carbonate mudstone from a 4800-m-thick composite sedimentary succession which provides a 12 Ma continuous record of environmental conditions during the early to middle Eocene (54 to 42 Ma). From the base of this record (at 54 Ma), oxygen isotopes ($\delta^{18}\text{O}$ values) show a faster decrease rate than the coeval global negative excursion associated with the Early Eocene Climatic Optimum (EECO). This local alteration of the global $\delta^{18}\text{O}$ signal indicates that topographic growth during this period, associated with significant tectonic activity, perturbed



the oxygen isotopic composition of foreland waters. Thus, our data suggest that significant topographic uplift of the Pyrenean orogen started from at least 54 Ma and continued until ca. 49 Ma, reaching the maximum elevations of 2000±500m in this phase from previous isotope and flexural studies. In addition, our record shows that the long-term carbon stable isotope composition during this period remained relatively stable with no similarity to the global bell-shaped long-term trend of the EECO. This is consistent with the restricted physiography of the South-Pyrenean foreland basin, mainly influenced by local sedimentary and water inputs. Overall, the Pyrenean topographic growth from the late Cretaceous to the Miocene displays several growth stages that seem to be primarily determined by episodes of increased rate of tectonic plate convergence. The duration of these growth stages (several millions of years) is a possible documentation of the response time of mountain ranges to tectonic perturbations. The results of this work therefore demonstrate that stable isotope measurements on whole-rock sediments in foreland basins can provide key information for tectono-climatic and topographic reconstructions of mountain ranges.

Introduction

Knowing the paleotopographic evolution of orogenic systems is key to understand the relationship between tectonics and surface processes, and their implications for the dynamics of sediment routing systems at geological timescales (e.g., Campani et al., 2012; Castelltort et al., 2015; France-Lanord et al., 1993; Romans et al., 2016; Sømme et al., 2009). In addition to acting as physical topographic barriers, orogens also impact atmospheric circulation and the transport of moisture, making the evolution of mountainous topographies an important factor in biodiversity evolution and adaptation (Hewitt, 2000; M.E. Raymo and W.F. Ruddiman, 1992; Mulch, 2016). The isotopic composition of oxygen ($\delta^{18}\text{O}$) preserved in sediments has been widely applied to reconstruct paleotopography and paleoelevation (e.g., Garzione et al., 2000, 2006; Rowley et al., 2001; Rowley and Garzione, 2007). Such approaches are based on principles linking the oxygen stable isotope composition of precipitation with elevation and “continentality” determined by a Rayleigh distillation process (e.g., Ambach et al., 1968; Dansgaard, 1964; Kukla et al., 2019; Siegenthaler and Oeschger, 1980). High topography and orographic precipitation induce isotopically lighter water (lower $\delta^{18}\text{O}$ values) in rainfall with a ratio of about 2.8 ‰ per km of elevation (Ambach et al., 1968; Poage and Chamberlain, 2001). For instance, the ca. -20 ‰ $\delta^{18}\text{O}$ value of precipitation measured in Himalayan catchments is significantly lower than their coastal counterparts of approximately -5 ‰ (Caves Rugenstein and Chamberlain, 2018; Cerling, 1984; Kukla et al., 2019). The $\delta^{18}\text{O}$ values can be measured in lacustrine and paleosol carbonates (e.g., Currie et al., 2005; Garzione et al., 2000, 2006), authigenic clay minerals (e.g., Chamberlain and Poage, 2000), mammalian tooth enamel (e.g., Fricke, 2003), or mollusk shells (e.g., Huyghe et al., 2012) deposited in basins adjacent to reliefs, making possible to reconstruct paleotopography from a broad variety of records.

65

Decades of study, and active ongoing research in the Pyrenean orogen have provided a comprehensive dataset about its tectonic and basin evolution (e.g., Chevrot et al., 2018; Grool et al., 2018; Macchiavelli et al., 2017; Puigdefabregas et al., 1986;



Rosenbaum et al., 2002; Vergés et al., 2002; Whitchurch et al., 2011). Moreover, several studies have obtained constraints on its topographic evolution through different methods such as flexural modelling (Curry et al., 2019; Millán et al., 1995) and pollen records (Ortuño et al., 2013; Suc and Fauquette, 2012), including $\delta^{18}\text{O}$ measurements (Huyghe et al., 2012, 2020; Zamarreño et al., 1997). Motivated by the issue of the post-tectonic topographic evolution of the Pyrenees, several works have focused on the appraisal of Miocene Pyrenean elevation (Huyghe et al., 2020; Ortuño et al., 2013; Suc and Fauquette, 2012; Tosal et al., 2021). The timing and magnitude of the topographic evolution of the orogen during its primary collisional history in the Late Cretaceous and Paleogene, have also received considerable attention. In a recent exhaustive exploration of flexural inversion of foreland stratigraphy, Curry et al (2019) have documented the significant topographic growth of the orogen that took place in the late Eocene-Oligocene, from ca 2000m of maximum elevation in the early-middle Eocene to 3000-3500 m by the end of the Oligocene. In addition, in agreement with tectonostratigraphic arguments and widespread evidence of a major phase of convergence in the lower Eocene (e.g., Puigdefabregas and Souquet, 1986; Puigdefabregas et al., 1992), earlier flexural inversion by Vergés et al (1995) and Millán et al (1995), as well as continental (Zamarreño et al., 1997) and marine (Huyghe et al., 2012) carbonate oxygen isotope compositions ($\delta^{18}\text{O}_{\text{carb}}$) data consistently indicate early topographic development of the range in the late Paleocene to middle Eocene. However, while these studies all suggest that the orogen reached 1000-2000 m of maximum elevation during this early stage of growth, the timing over which this growth took place remains largely undetermined, within a possibly greater than 10 My window. Resolving such uncertainty is important to draw a complete picture of the topographic history of the Pyrenees and address its relationships with tectonics and climate.

85

The objective of the work presented here is to generate an extensive dataset of stable oxygen isotope composition of carbonates in the South-Pyrenean foreland basin, encompassing the early to middle Eocene. This should test and/or provide additional constraints on a possible significant topographic growth during the early Eocene and place this important tectonic and basin reconfiguration period within the evolution of the Pyrenees, from its initiation in the upper Cretaceous to the end of convergence in the Miocene. Finally, results of this study might allow discussing the respective roles of climate and tectonics on the topographic evolution of a mountain range.

90

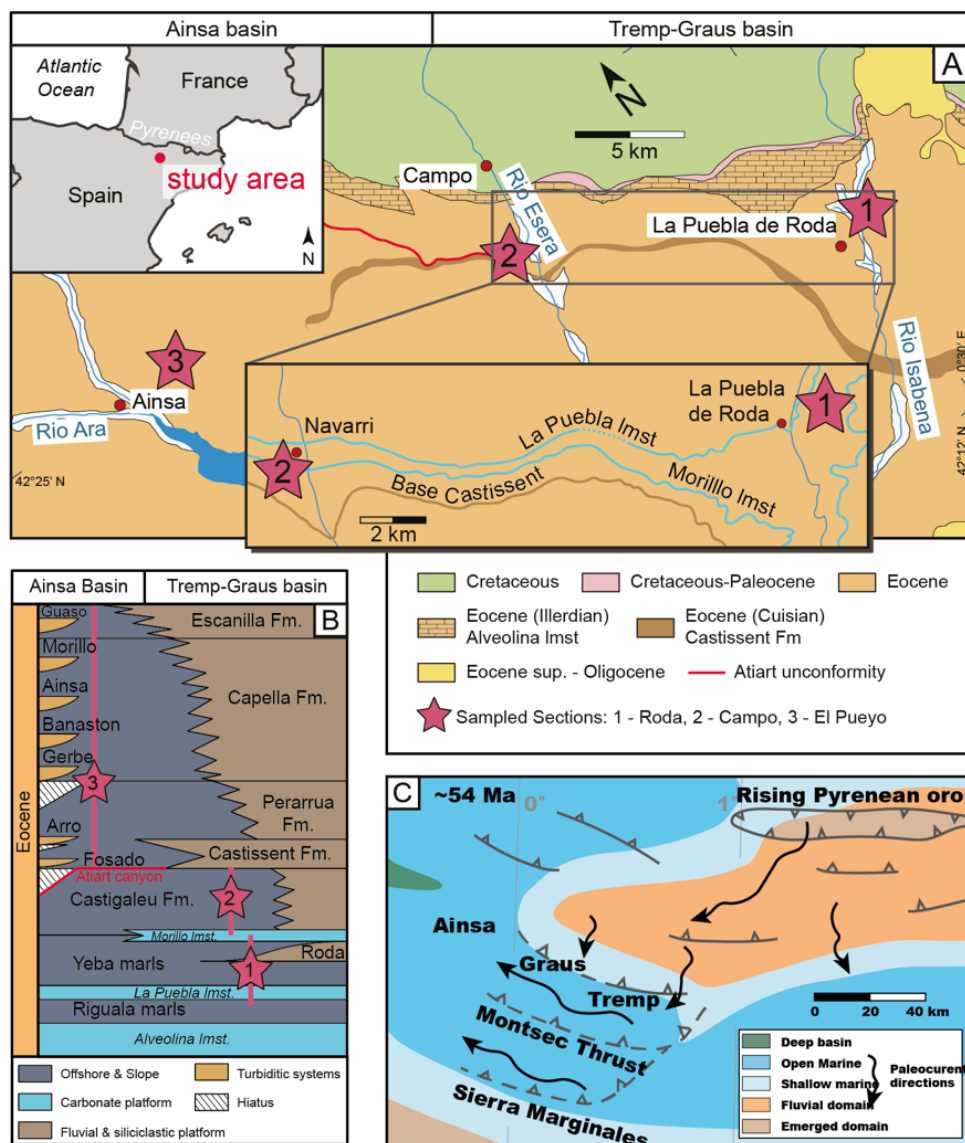


Figure 1 – Study location with stratigraphic and paleogeographic context of sampled material. A - Simplified geological map of the study area showing the situation of sections 1, 2 and 3. Map based on the Mapa geològica de Catalunya (1:300 000, Institut Geològic and Institut Cartogràfic de Catalunya). Inset zoomed on the marker beds Morillo and La Puebla limestones (after Bentham and Burbank, 1996) used for physical correlation of sections 1 and 2. B - Chrono-litho-stratigraphic diagram of the Tremp–Graus and Ainsa Basins during the Eocene with location of the sampled sections (after Chanvry *et al.*, 2018). The diagram highlights the progradation from East (Tremp–Graus Basin) to West (Ainsa Basin) of the clastic systems, and the paleogeographic situation of the sections sampled in a proximal-distal profile. C – Paleogeographic map of the South-Pyrenean basins during the late Paleocene – early Eocene at ~54 Ma from Vacherat *et al.* (2017) and location of the Tremp and Ainsa basins.



Pyrenean tectonic and climatic framework

Tectonic evolution

The Pyrenees are an E-W-oriented orogen that developed from the Upper Cretaceous to the Miocene due to the convergence between the Iberian and Eurasian plates (Choukroune, 1989; Muñoz, 1992; Puigdefabregas et al., 1992; Séguret, 1972). With the onset of convergence, thrust-related exhumation started in the eastern Pyrenees during the Late Cretaceous (Fig. 2, e.g., Puigdefabregas and Souquet, 1986; Filleaudeau et al., 2012; Mouthereau et al., 2014; Ternois et al., 2019; Thomson et al., 2017; Vacherat et al., 2017; Whitchurch et al., 2011). In the South-Pyrenean basin, sediments were sourced mainly from the south-east, and fed the Tremp-Graus sub-basin until the late Maastrichtian (Gómez-Gras et al., 2016). At this time, the early Pyrenean orogenic wedge was overall submarine (Ford et al., 2016). Exhumation rates increased from ~0.5 to 0.8 mm/yr in the eastern Pyrenees from the late-Cretaceous to the Paleocene (Whitchurch et al., 2011). Moreover, thermochronological data suggest that in the Northeastern Pyrenees, the Agly and Salvezine massifs were close to the surface between the late-Cretaceous and early Paleocene (Ternois et al., 2019). Subaerial topography, if present, was thus limited to the eastern sector of the Pyrenees. However, most of this area has been dismantled during the subsequent Neogene opening of the Gulf of Lions (Gunnell et al., 2008; Huyghe et al., 2020), such that the paleo-elevation reached by these relief remains difficult to determine in the absence of nearby sedimentary records.

The Paleocene is considered as a period of relative tectonic quiescence in the northern and southern Pyrenean basins (Rosenbaum et al., 2002; Ford et al., 2016; Whitchurch et al., 2011), with convergence rates between Eurasia and Iberia of ca. 0.8 mm/yr, (Macchiavelli et al., 2017; Rosenbaum et al., 2002) and shortening rates of less than 0.5 mm/yr (Fig. 2, Grool et al., 2018; Vergés et al., 2002). Motion between plates resumed with significantly higher rates (3.2 mm/yr) during Ypresian to Lutetian times (Macchiavelli et al., 2017; Rosenbaum et al., 2002). The Ypresian period in particular, encompassing the Early Eocene Climatic Optimum (EECO), is associated with high rates of shortening (4-4.4 mm/yr, Grool et al., 2018; Vergés et al., 2002) coeval with a major pulse of exhumation of the Axial Zone at ca. 50 Ma (Fig. 2, Beamud et al., 2011; Fitzgerald et al., 1999; Thomson et al., 2020; Whitchurch et al., 2011) and a major phase of foredeep subsidence in the Jaca and Ripoll basins (Garcés et al., 2020). This is also associated with an increase of clastic supply from the growing orogen and the initiation of the progradation of large siliciclastic systems such as recognized for instance in the Ypresian Roda, Castigaleu and Castissent fluvio-deltaic formations (Fig. 1, Castelltort et al., 2017; Chanvry et al., 2018; López-Blanco et al., 2003; Odlum et al., 2019; Puigdefabregas et al., 1986; Thomson et al., 2019). During the Lutetian, the shortening rate of the Pyrenees decreased and remained nearly constant at 1.5-2.6 mm/yr until the Oligocene (Grool et al., 2018; Vergés et al., 1995, 2002). It is estimated that most of the Pyrenean mountain range was subaerial by the end of the Lutetian (e.g., Vacherat et al., 2017). Another important increase in tectonic activity, with exhumation rates from 3 to 4 mm/yr, occurred during the late Eocene to Oligocene as shown by apatite and detrital zircon fission track analysis (Fig. 2, Beamud et al., 2011; Metcalf et al., 2009; Morris et al., 1998; Whitchurch et al., 2011) and by 3D numerical modelling of orogenic loading and flexure (Curry et al., 2019). This was



paired with the closure of the marine South-Pyrenean foreland basin at ca. 36 Ma (Costa et al., 2010) which led to widespread
135 piedmont aggradation (e.g., Babault et al., 2005) and topographic development to maximum elevations similar to the present-
day (Curry et al., 2019). Eventually, convergence between Iberia and Europe slowed to 0.2 mm/yr in the earliest Miocene
(Macchiavelli et al., 2017) and orogenic growth nearly stopped (Fillon and van der Beek, 2012). Although we do not address
this issue in the present work, it is worth mentioning that the elevation reached by the Pyrenees in the Miocene is the subject
of ongoing debate between a number of tectonosedimentary observations (Puigdefàbregas et al., 1992) and recent
140 paleobotanical reconstructions (Tosal et al., 2021), which suggest that the Eastern Pyrenees were at similar or higher elevations
than present-day, and other palynological and isotope data, which advocate for a period of topography decay in the Miocene
followed by uplift associated with volcanism and limited to the eastern Pyrenees during the late Miocene (Gunnell et al., 2008;
Huyghe et al., 2020; Ortuño et al., 2013; Suc and Fauquette, 2012).

Global and regional climate

145 During the Eocene (56 to 33,9 Ma), Earth reached its warmest climate of the last 66 Ma (e.g., Zachos et al., 2001, Fig. 2). The
EECO (Early Eocene Climatic Optimum), broadly situated between 53.3 and 49.1 Ma (Westerhold et al., 2018), marks the
culmination of this warm period and is characterized by a long-term decline in $\delta^{18}\text{O}$ and $\delta^{13}\text{C}$ values with an overall minimum
at ca. 51.3 Ma (Fig. 2, Cramer et al., 2009). The end of the EECO marks the beginning of the transition from the Eocene
greenhouse to the present icehouse period with the progressive establishment of permanent Antarctic ice sheets since the
150 Eocene-Oligocene boundary (Miller et al., 1991; Zachos et al., 2008).

In the Pyrenees, Payros et al. (2015) identified the EECO in oxygen isotopes of a deep-marine succession deposited in the
early Eocene Basque Basin and extracted a multiproxy record of increased rainfall, runoff and continental weathering. This is
in agreement with palynological data from the South-Pyrenean foreland basin which suggest an increase in temperature
155 culminating between 52 and 48 Ma and decreasing afterwards (Haseldonckx, 1973). At 50 Ma, during the EECO, Mean Annual
Precipitation estimates (Sheldon et al., 2002), together with the presence of iron-oxides and hydroxides nodules described in
the Castissent Formation suggest a semi-arid to sub-humid climate with seasonal humidity (Honegger et al., 2020).

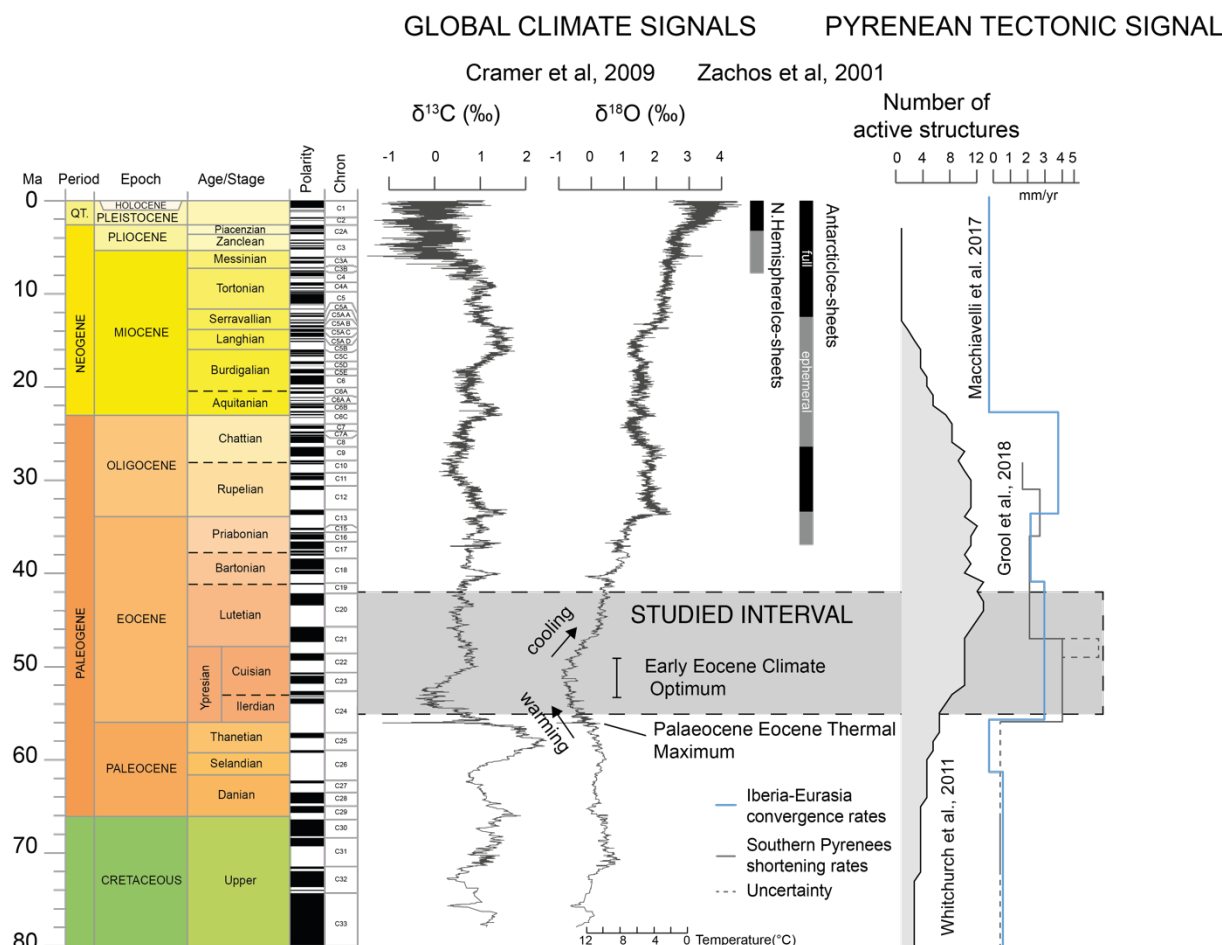


Figure 2 : Global climatic and Pyrenean tectonic signals of the past 80 Ma. The tectonic signal is represented by the estimated rates of convergence and shortening, and by the cumulative number of active structures (from Whitchurch et al., 2011). The climatic signal is represented by Zachos et al (2001) $\delta^{18}\text{O}$ and Cramer et al (2009) $\delta^{13}\text{C}$ compilations. MECO: middle Eocene climatic optimum. EECO: early Eocene climatic optimum. PETM: Paleocene-Eocene thermal maximum. Peak exhumation periods from Whitchurch et al. (2011). All information scaled to GTS2012. Modified after Clark et al (2017).

Material and methods

Sampling

A total of 658 samples were collected on three correlated and partially-overlapping sedimentary sections from the Tremp-Graus and Ainsa sub-basins (Fig. 1), which together build a continuous stratigraphic record from lower Ypresian to upper Lutetian. Magnetostratigraphic constraints (Bentham and Burbank, 1996; L  uchli et al., 2021) on all sections provide robust time lines for correlation with global target isotopic profiles. In order to avoid the possible influence of differential lithology and depositional conditions on the isotopic composition of bulk carbonates, all samples consist of marine carbonate mudstone deposited in prodeltaic to upper-slope environments in depositional water depths estimated between few tens (Roda carbonate



marls, e.g., López-Blanco et al., 2003) and a few hundreds of meters (Ainsa basin, Fosado and Arro slope carbonate marls, e.g., Pickering and Corregidor, 2005).

- 175 The base of our record is at the La Puebla Limestone (Fig. 1) formation, which crops out in the Isábena river valley (Bentham and Burbank, 1996 and mapping by C. Puigdefábregas in Clark et al., 2017) and marks the base of the Roda section (section number 1, Fig. 1). The Morillo limestone, situated at the top of the Roda section, can be mapped to the adjacent Ésera river valley in the West (Bentham and Burbank, 1996; Nijman, 1998), where marks the basis of the Campo section (section number 2, Fig. 1). The western flank of the Ésera valley marks the transition to deeper-water environments of the Hecho Group (Mutti, 180 1977). A large-scale erosion feature (Atiart canyon), equivalent with the base of the Castissent fluvial formation in the Ésera valley, allows correlation with the deeper basin as it marks the base of the Hecho Group in the El Pueyo section (section number 3, Fig. 1) (Mutti et al., 1988).

Stable isotopes

- Between 150 and 300 µg of whole marine carbonate mudstone were crushed and powdered in an agate mortar and analysed for stable carbon and oxygen isotope composition at the Institute of Earth Surface Dynamics of the University of Lausanne (Switzerland) using a Thermo Fisher Scientific (Bremen, Germany) carbonate-preparation device and Gas Bench II connected to a Thermo Fisher Delta Plus XL isotope ratio mass spectrometer. The carbon and oxygen isotope compositions are reported in the delta (δ) notation as the per mil (‰) isotope ratio variations relative to the Vienna Pee Dee Belemnite standard (VPDB). The standardization of the $\delta^{13}\text{C}$ and $\delta^{18}\text{O}$ values relative to the international VPDB scale was performed by calibration of the reference CO_2 gas and working standard with international reference materials NBS 18 (carbonatite, $\delta^{13}\text{C} = -5.01$ ‰, $\delta^{18}\text{O}_{\text{VPDB}} = -23.01$ ‰) and NBS 19 (limestone, $\delta^{13}\text{C} = +1.95$ ‰, $\delta^{18}\text{O}_{\text{VPDB}} = -2.2$ ‰) (values from Brand et al., 2014). The analytical reproducibility (1 sigma) estimated from replicate analyses of the international calcite standards and the laboratory standard Carrara Marble ($\delta^{13}\text{C} = +2.05$ ‰, $\delta^{18}\text{O}_{\text{VPDB}} = -1.7$ ‰) was better than ± 0.05 ‰ for $\delta^{13}\text{C}$ and ± 0.1 ‰ for $\delta^{18}\text{O}$. 190

Organic matter

- Organic matter (OM) analyses (Fig. 3) were performed on 379 of our samples in the most proximal (Roda, section number 1, Fig. 1) and most distal (El Pueyo, section number 3, Fig. 1) sections, using a Rock-Eval 6 at the Institute of Earth Sciences of the University of Lausanne, following the method described by Espitalie et al. (1985) and Behar et al. (2001). Measurements were calibrated using the IFP (Institut Français du Pétrole) 160000 standard. We use the Rock-Eval pyrolysis to assess the total organic-carbon content (TOC, wt.%), hydrogen index (HI, mg HC/g TOC, HC = hydrocarbons), oxygen index (OI, mg CO_2 /g TOC) and T_{max} (°C), which together characterize the preserved organic matter in terms of amount, nature (source), and thermal maturity (e.g., Espitalie et al., 1985) and can be interpreted as proxies of environmental and basin evolution. HI, OI and T_{max} values were interpreted for TOC ≥ 0.2 wt.% and S2 values ≥ 0.2 mg HC/g, after a careful check of the corresponding pyrograms. 200



Sediment budget in the South-Pyrenean foreland basin

205 A conservative (minimum) estimate of sediment flux coming from the mountain belt can be obtained from preserved volumes of sediments in the Foreland basin. Several studies have focused on those quantifications in the south-Pyrenean Foreland basins, Ebro and Duero basins (Alonso et al., 1996; Filleaudeau, 2011; Garcia-Castellanos et al., 2003; Sinclair et al., 2005) and also in the adjacent Valencia basin (Arche et al., 2010; Garcia-Castellanos et al., 2003; Watts and Torné, 1992a). These studies are based on the compilation of seismic and wells data available in the basins. We here only report the total volumes of preserved sediments obtained from Filleaudeau (2011). The amount of in-situ biogenic carbonates and evaporites is considered a minor fraction of the dominantly clastic composition of the foreland successions of the South-Pyrenean deposits, and has thus not been corrected from the estimates presented in this work. In addition, the estimates of Filleaudeau (2011) also were not decompacted, which may lead to overestimation of volumes of the upper part of the sedimentary fill with respect to its lower part. In summary, the evolution of estimated preserved volumes in the South-Pyrenean foreland basin presented here is preliminary and of indicative nature only.

Comparison with global records

The stack of new isotopic data obtained here and composing a nearly complete early Eocene profile of stable carbon and oxygen isotopes is compared with the global benthic isotopic compilation of Cramer *et al* (2009) with timescale updated to the Global Time Scale GTS2012. To compare both profiles, we use the Analyseries software of Paillard et al. (1996) and tie-lines given by the magnetic reversals of magnetochrons C24n to C19r identified on the Roda, Campo and El Pueyo sections (Benthams and Burbank, 1996; L  uchli et al., 2021). The resulting correlation is consistent with previous biostratigraphic dating in the Hecho Group (Scotchman et al., 2015).

Results and discussion

Absolute values and diagenetic overprint

225 The measured $\delta^{13}\text{C}$ and $\delta^{18}\text{O}$ values in all sections presented here (Fig. 4) are all considerably lower, i.e. $\sim 5\text{‰}$ and $\sim 2\text{‰}$ more negative in oxygen and carbon respectively, than their time-equivalent fresh benthic counterparts (Fig. S1 and S2, Cramer et al., 2009). This suggests that, although they may contain a primary record of the early–middle Eocene evolution, their absolute values could have been altered as in other paleogene isotopic datasets in the Pyrenean domain (Castelltort et al., 2017; Molina et al., 2003; Payros et al., 2015; Schmitz et al., 2001). The HI- T_{max} relation (Fig. 3) shows that the samples from the Roda section are mostly in the immature zone (i.e., below 60 °C, Machel et al., 1995) of low diagenesis level, and that samples from the El Pueyo section are mostly in the oil window suggesting burial temperatures of ca. 80–100 °C (Machel et al., 1995) and thus underwent medium diagenetic overprint (Espitalie et al., 1985). T_{max} values increase with depth for the first ca. 3500 m of the El Pueyo section (Fig. 4), consistent with ~ 4 km of overburden in the Ainsa basin (e.g., Heard et al., 2008). However,



we observe that T_{\max} values in the lowest 500 m of the same El Pueyo section decrease with depth back to values similar to those found at the top of the succession (Fig. 4). Moreover, the global $\delta^{18}\text{O}$ profile of Cramer et al. (2009) shows similar correlation of $\delta^{18}\text{O}$ with depth for the El Pueyo interval ($r = 0.82$ and 0.83 for the global and Pyrenean records respectively, Fig. S3), suggesting that the covariant decline of $\delta^{18}\text{O}$ and increase of T_{\max} with depth on El Pueyo section are unrelated, i.e. that the $\delta^{18}\text{O}$ trend rather reflects a primary signal similar to its global equivalent. Low T_{\max} values in the Roda section (Fig. 4) imply relatively low burial-depth and diagenetic overprint, which can be extrapolated to the Campo section, which belongs to the same structural sector (Trempe-Graus sub-basin, Fig. 1) and involves similar sedimentary thicknesses (Chanvry et al., 2018). Lastly, cross-plots of $\delta^{13}\text{C}$ and $\delta^{18}\text{O}$ show no systematic covariances between both stable isotope systems, with Pearson coefficients of 0.48 , 0.61 , -0.03 and 0.26 for the El Pueyo, Campo, Roda, and combined sections respectively (Fig. S4), thus also suggesting limited diagenetic influence (Marshall, 1992).

Carbon isotope evolution

The bulk $\delta^{13}\text{C}$ data (Fig. 4C) show significant spread with a mean moving standard deviation of $1\sigma = 0.53\text{‰}$ (1 Ma window). This dispersion is particularly important when compared to the magnitude of change of $\delta^{13}\text{C}$ in the global ocean over the same period (0.24‰), and it may thus mask climate-controlled $\delta^{13}\text{C}$ signals such as hyperthermal events occurring during this interval of the Cenozoic (e.g., Westerhold et al., 2018). Such spread can be attributed to the restricted physiography of the South-Pyrenean foreland basin and its proximal position to the rising orogen, which may have hindered exchange and equilibration (Saltzman and Thomas, 2012) with the open ocean, by frequent injections of very negative $\delta^{13}\text{C}$ waters due to oxidation of organic matter (Jenkyns, 1996; Kroopnick, 1985) of mainly terrestrial origin (type III), as evidenced in the Hydrogen Index (HI, HC/g TOC) and Oxygen Index (OI, mg CO_2 /g TOC) from the El Pueyo and Roda sections (Fig. 3).

Oxygen isotope evolution and topography

Measured $\delta^{18}\text{O}$ values show a bell-shaped evolution with a decline from -4.7‰ to -7.0‰ in the first 2'000 m of the section, followed by an increase back to -4.5‰ at the top of the record (Fig. 4), and little dispersion with $1\sigma = 0.29\text{‰}$ of moving standard deviation (200 m window).

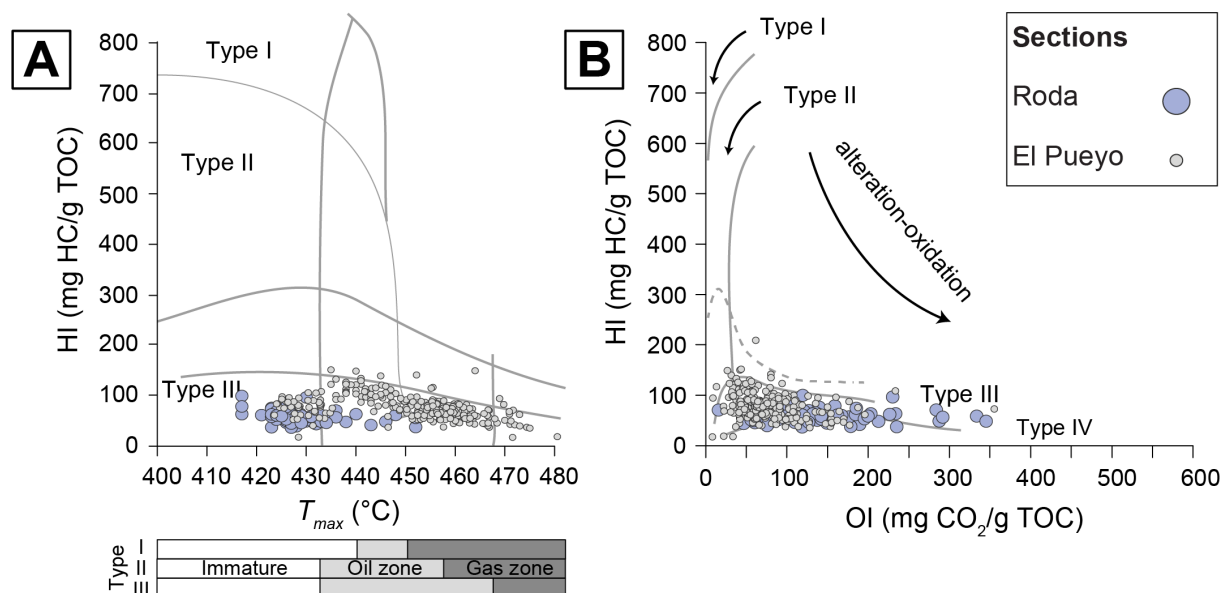


Figure 3 - HI v. T_{max} and HI v. OI plots of the Roda (section 1, Fig. 1) and El Pueyo (section 2, Fig. 1) sections. HI- T_{max} relation shows that the samples from the Roda section are mostly in the immature zone, and that samples from the El Pueyo section are mostly in the oil window suggesting low and medium diagenetic overprint respectively.

260

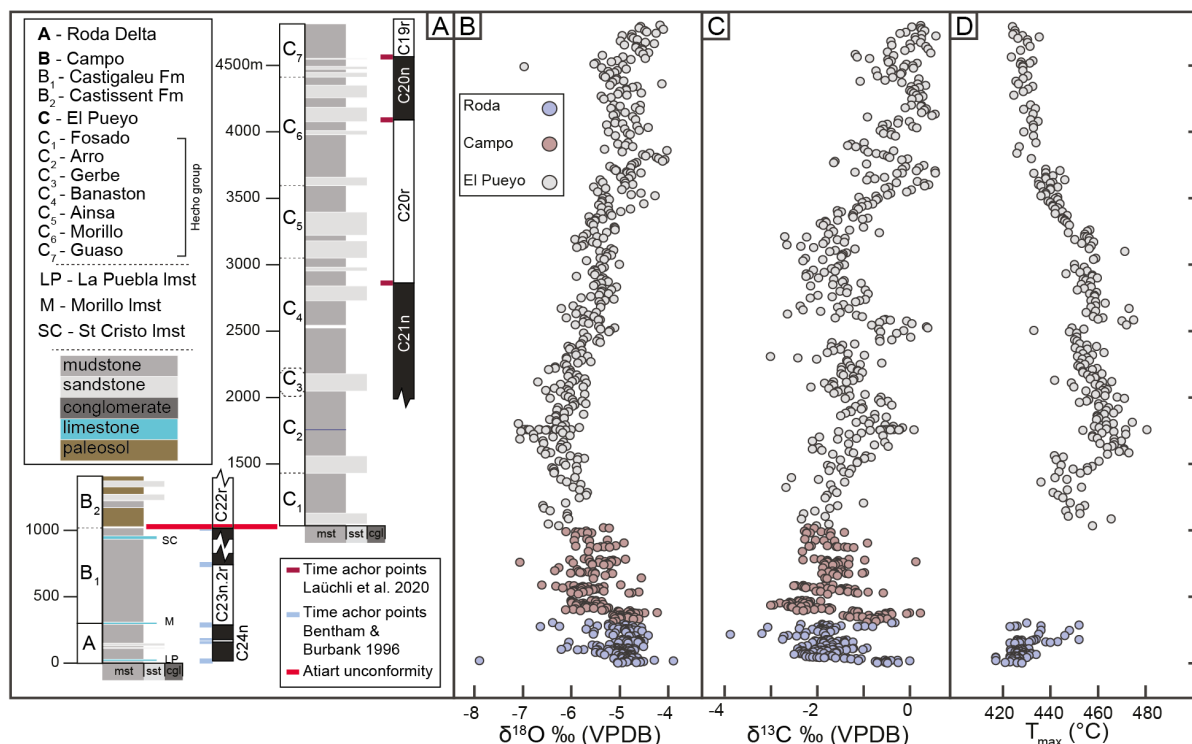


Figure 4 – Oxygen (B) and carbon (C) isotopic record, and T_{max} (D) values of samples measured from the Roda-Campo-El Pueyo composite section (A). Magnetostratigraphic anchor points from Bentham and Burbank, 1996 and Laüchli et al., 2021).



265

Despite the difference in absolute values, this pattern of bell-shaped evolution is similar to the global $\delta^{18}\text{O}$ record of Cramer et al (2009) (Fig. 2, 5, S2, and S3). This shows values evolving from -0.5‰ to -1.3‰ in the early Eocene paired with global warming of the EECO (corresponding to an increase in global temperature from ca. 9.5 to 12 °C, Zachos et al., 2001) and followed by values increasing from -1.3‰ to 0.5‰ during the subsequent global cooling (Fig. 2 and 5, ca. 12 to 6.5°C, Zachos et al., 2001). However, a locally weighted linear regression shows that the measured $\delta^{18}\text{O}$ reaches minimum values (below 97th percentile) between 49.4 and 49.0 Ma, i.e. ca 2.1 Ma later in the Pyrenean succession than in the deep-sea global record, where it occurs at 51.3 ± 0.2 Ma (lower 97th percentile). In addition, the rate of decline of $\delta^{18}\text{O}$ before 51.3 ± 0.2 Ma is 3 times higher in the Pyrenean record than in the global profile (Fig. 5).

275

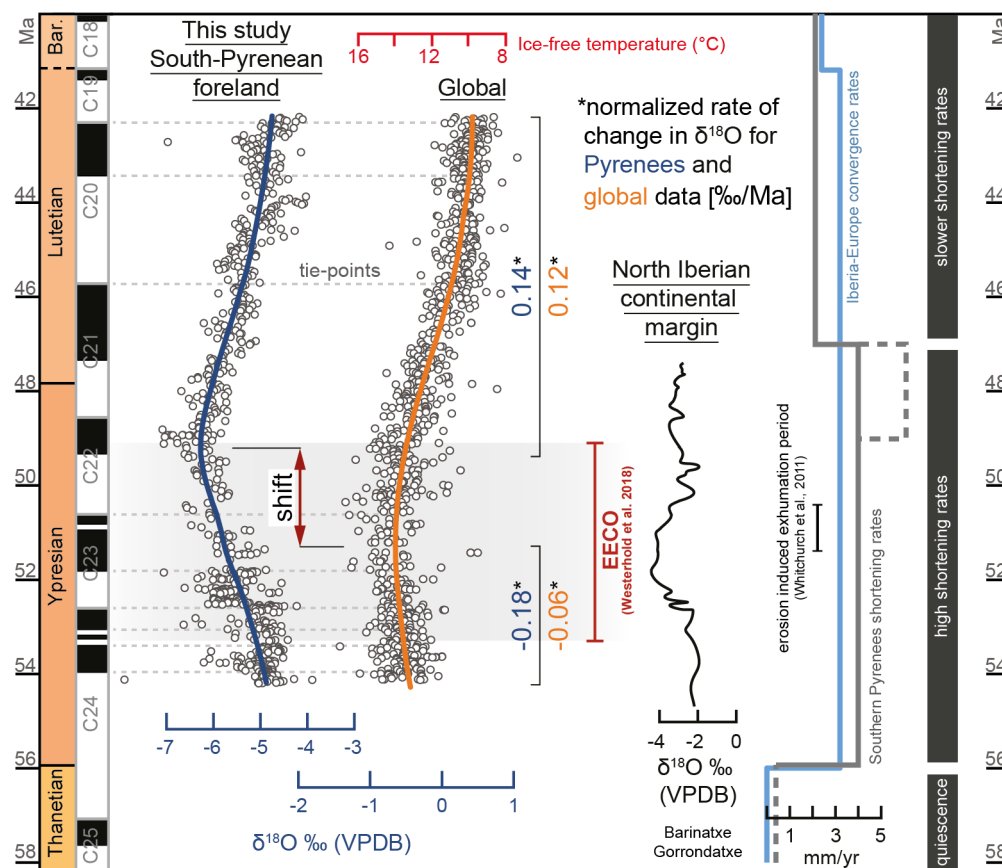


Figure 5 – Comparison between South-Pyrenean (blue, left), global (orange, middle) and North Iberian (right, bold) continental margin $\delta^{18}\text{O}$ records. $\delta^{18}\text{O}$ global record from Cramer et al. (2009), north Iberian continental margin $\delta^{18}\text{O}$ record from Payros et al. (2015). Pyrenean shortening rates from Grool et al. (2018), Iberia-Europe convergence rates from Macchiavelli et al. (2017). EECO extension from Westerhold et al. (2018). Compared with the global benthic record (orange profile, middle), the oxygen isotope



280 evolution of the Pyrenean carbonates (blue profile, left) shows a four times greater rate of decline towards negative values in the early Eocene, and reaches peak minimum at ca. 49 Ma, i.e. ca. 2 Ma later than peak global minimum of the EECO at 51 Ma.

Aside from diagenetic effects, the $\delta^{18}\text{O}$ signature of carbonates depends primarily on the temperature of calcification (related to water temperature in the environment), and on the $\delta^{18}\text{O}$ of the surrounding water ($\delta^{18}\text{O}_w$), which is in turn dependent on the
 285 mixing of global and local waters as well as salinity and evaporation (Garzione et al., 2004; Pearson, 2012).

The 2.1 Ma lag in the measured $\delta^{18}\text{O}$ minimum values identified here is not observed in coeval measured $\delta^{18}\text{O}$ in the Barinatxe-Gorrondatxe section (Fig. 5, Payros et al., 2015) ca. 200 km west of the study area, suggesting that our observation could imply a local warming, limited to the central part of the South-Pyrenean foreland basin, yet sustained for ~2 Ma. Although there might have been some latitudinal diachrony in the onset and end of the EECO warming event (Payros et al., 2015), the globally-
 290 homogeneous climate and reduced latitudinal gradient of the EECO period (Andreasson and Schmitz, 2000) rather excludes the long-term presence of a local temperature difference of several degrees for 2.1 Ma in such a spatially-limited area. We therefore consider unlikely the possibility that warming continued in the Pyrenees until 49.2 Ma while cooling already started globally 2.1 Ma earlier.

295 Alternatively, we here hypothesize that the perturbation of the $\delta^{18}\text{O}$ signal in the South-Pyrenean foreland basin observed in these data primarily signals the major topographic development of the mountain range between ca. 54 and ca. 49 Ma. Hereinafter we describe the two main processes that support this hypothesis.

First, the increase of the mean elevation of the Pyrenees during that period, would deliver increasingly negative $\delta^{18}\text{O}$ waters
 300 to the basin, because oxygen isotopic composition of precipitation decreases with increasing elevation through Rayleigh distillation process during orographic rainout (e.g., Caves Rugenstein and Chamberlain, 2018; Poage and Chamberlain, 2001; Rowley and Garzione, 2007). Huyghe et al (2012) demonstrated with a morphological-hydrological model that such process could explain the negative offset between $\delta^{18}\text{O}$ values measured on early to middle Eocene mollusc shells in the South-Pyrenean foreland basin and those recorded in coeval deposits of the Paris basin. Our extensive dataset spanning a longer (12
 305 Ma) and denser (658 measurements) record than previously presented by Huyghe et al. (2012) (5 Ma and 12 measurements) suggests that the phenomenon identified by their study may have been effective already at 54 Ma and continued until 49 Ma. By constantly adding negative $\delta^{18}\text{O}$ waters to the restricted foreland reservoir, and assuming hindered mixing and equilibration of the restricted Tremp-Graus and Ainsa sub-basins (also presumably increasingly restricted with ongoing shortening) with the global ocean, the growth of the orogen steered the local $\delta^{18}\text{O}$ composition of foreland carbonates towards more negative
 310 values at a faster pace than the global trend and forced a perpetuation of this trend during ca. 2 Ma longer than in the global oceanic reservoir. A higher Pyrenean topographic development, via surface drainage area expansion and elevation growth (mean and maximum), imposed an increasingly higher discharge of increasingly negative (isotopically light) $\delta^{18}\text{O}$ waters to



the immediately adjacent foreland basin, which superimposed on the global $\delta^{18}\text{O}$ decrease and forced the divergence of the two $\delta^{18}\text{O}$ profiles (local and global, Fig. 5).

315

Second, nearshore and relatively enclosed environments are strongly influenced by freshwater input and evaporation effects. Since $\delta^{18}\text{O}$ increases with salinity by approximately 0.2‰/psu (1 psu = 1 g of NaCl per kg water, Maclachlan et al., 2007; Marshall, 1992) a higher proportion of freshwater input in the relatively confined South-Pyrenean foreland basin during Eocene times (Vacherat et al., 2017) could potentially be the cause of the local lower (more negative) $\delta^{18}\text{O}$ values. An input of
 320 freshwater shifting the $\delta^{18}\text{O}$ minimum from -5.5 ‰ at 52 Ma to -6.5 ‰ at 49 Ma would imply a change in salinity of ca. 5 psu during this period. This is roughly the difference between two contrasted marine environments such as mean proximal Bengal Bay (31 psu, Akhil et al., 2016) and mean Atlantic salinity values (35 psu, Le Vine et al., 2007). Past salinity is difficult to constrain (Huyghe et al., 2012), but a decrease in salinity due to freshwater input alone would imply a relative salinity change equivalent to an environmental change from proximal to open ocean in the South-Pyrenean foreland basin. Developing
 325 a mixing model of freshwater input and oceanic boundary conditions to assess the resulting composition of basin waters would require constraining not only the precipitation regime but also the size of drainage areas and the physiographic configuration (areal and bathymetric) of the receiver basin. These constraints are beyond the scope of the present work but certainly highlight the need for further research and modeling to assess the local distortion of isotopic proxies by tectonically-induced topography. Nevertheless, the effect of increasing freshwater on the local decrease in salinity may have exacerbated the divergence between
 330 the local and global $\delta^{18}\text{O}$ records.

After the $\delta^{18}\text{O}$ minimum values at ~ 49 Ma, the $\delta^{18}\text{O}$ preserved in the South-Pyrenean foreland basin shifts back towards more positive values with a normalized rate of 0.14‰ per Ma comparable to that of the global $\delta^{18}\text{O}$ record over the same period (0.12 ‰/Ma). The evolution of $\delta^{18}\text{O}$ in the Pyrenees between 49 and 42 Ma mirrors the post-EEOCO global increase in $\delta^{18}\text{O}$
 335 values towards cooler climatic conditions (Cramer et al., 2003). This indicates that topographic expansion and elevation change of the orogenic domain, if they took place, did not perturb the isotopic signal in the same way as they did between 54 and 49 Ma. Since previous studies consistently point out stable shortening and convergence rates from 49–47 Ma to at least 42 Ma (Fig. 5, Machiavelli et al., 2017; Grool et al., 2018; Vacherat et al., 2017; Vergés et al., 1995), we interpret this lack of perturbation of the $\delta^{18}\text{O}$ profile as consistent with negligible topographic growth from 49 to 42 Ma (our youngest data point).

340 **A composite narrative of Cenozoic Pyrenean topographic development**

Comparing the oxygen stable isotopic signature of molluscs between the South-Pyrenean foreland basin and the stable Paris basin, Huyghe et al. (2012) estimated that the Pyrenees had reached an elevation of 2000 ± 500 m between 49 and 41 Ma. Our data indicate that the Pyrenees grew between 54 and 49 Ma (2nd growth period on Fig. 6) and then remained relatively stable until 42 Ma. Based on oxygen isotopic composition of fluvio-lacustrine stromatolites, Zamarreño et al (1997) suggest early
 345 Eocene change in altitude of the Ebro basin margin (Catalan Coastal Ranges) of the order of 1000m, followed by no further



change until mid-upper Eocene. Taken together, these converge toward suggesting a ca. 1000 m topographic development of the Pyrenees during the early Eocene, followed by relatively stable elevation until middle-upper Eocene.

Curry et al. (2019), based on flexural-modeling scenarios matching topographic loads and South-Pyrenean foreland basin stratigraphy, found a significant increase of topography from the Bartonian to the end of the Eocene (ca. 41-34 Ma, Fig. 6), i.e. after the period investigated in the present work, and that topography then remained relatively stable since the end of the Eocene (Fig. 6) (Curry et al., 2019). These constraints combined with our findings suggest that Pyrenean topography developed in a punctuated manner, alternating periods of topographic growth and periods of topographic stability/quiescence. A first period (Fig. 6) of topographic development, with an emerged topography limited to the eastern Pyrenees, took place in the early stages of collision (Santonian to Paleocene, e.g., Puigdefabregas and Souquet, 1986), and was followed by a period of topographic quiescence during the Paleocene (Rosenbaum et al., 2002). A second period of topographic development occurred in the early Eocene and lasted until ca. 49 Ma (this study and Huyghe et al., 2012), followed by a second period of stability (2nd period of growth and stability on figure 6). The last period of growth took place in the middle Eocene and lasted until the end of the Eocene to early Oligocene, when it was in turn followed by a period of relative stability according to Curry et al (2019).

Tectonics, climate and topography

In Figure 6 we show a comparison between the history of Pyrenean topographic growth documented here, with global climatic records provided by the $\delta^{18}\text{O}$ record of ocean temperature (Zachos et al., 2001; Cramer et al., 2009) and global sea-level change (e.g. Kominz et al., 2008), as well as with regional plate dynamics (Iberia-Eurasia convergence, e.g. Machiavelli et al., 2017), regional deformation (shortening rates in the Pyrenean domain, Grool et al., 2019), and exhumation (Whitchurch et al., 2001).

Climate

We observe that the two periods of major topographic growth documented in the Pyrenees, in the early Eocene (54-49 Ma) and late Eocene-Oligocene (41-34 Ma), do not show a consistent correlation with climate. Indeed, the early Eocene topographic growth took place in a period of global warming that initiated in the Paleocene and culminated in the Ypresian (early Eocene) at ~50 Ma (EECO). On the contrary, the next period of major topographic development (Fig. 6) occurred within the global cooling trend of the middle to late Eocene, which is notably marked by the development of Antarctic ice sheets at the Eocene-Oligocene transition (EOT, Zachos et al., 2001).

Models of erosion and sediment transport generally consider a positive relationship between mean temperature, precipitation and global erosional efficiency through weathering and runoff-discharge dependent incision and transport (e.g., Tucker and Slingerland, 1997). Assuming such a positive relationship between climate (“climate” being here considered as the mean values of temperature and precipitation) and erosional efficiency, landscape evolution models (e.g., Whipple, 2001; Bonnet and Crave, 2003; Whipple and Meade, 2006) usually predict that the “topography” of a steadily uplifting orogen would decrease



with increased erosional efficiency during climate warming, such as in the early Eocene, and would be accompanied by a
 380 transient pulse in sediment flux out of the orogen. Conversely, the topography would be predicted to increase with cooling,
 such as during the mid-late Eocene, and be accompanied by a transient decrease of sediment flux out of the orogen. Despite
 the broadly indicative nature of the sediment accumulation data presented here, both periods of topographic growth
 documented in this work are accompanied by important increase of sediment supply to the south-Pyrenean basin (Fig. 6).
 Therefore, the early Eocene period (54–49 Ma) is consistent with climate-controlled erosion in terms of sediment flux out of
 385 the orogen (flux increases is consistent with more erosive climate with warming), but not in terms of topographic growth (more
 erosive climate should induce topographic decline). On the other hand, the late Eocene topographic growth (41–34 Ma) is
 consistent with a shift towards less erosive climate, but inconsistent in terms of sediment flux (topographic growth induced by
 less erosive climate should manifest itself by a decrease of sediment flux out of the orogen).

390 In the following, we present and discuss the more straightforward link that is manifest between topographic growth, sediment
 flux, and tectonics.

Tectonics

The Pyrenean tectonic evolution documented here shows that periods of topographic growth are consistent with periods of
 395 increased convergence between plates (Fig. 6), and periods of topographic stability occur during intervals of more constant
 plate convergence. First, at 56 Ma, the convergence rate between Iberia and Europe records an important increase from near
 zero in the Paleocene to 3.2 mm/yr in the Eocene (Macchiavelli et al., 2017). This major perturbation of the boundary
 conditions marks an acceleration of Pyrenean mountain building and is expressed by a fourfold increase of shortening rates in
 the South Pyrenees, from 1 mm/yr to 4 mm/yr (Grool et al., 2018; Vergés et al., 2002), a ca. twofold increase in the number
 400 of recorded active structures (Clark et al., 2017) and a pulse of exhumation centered at ca. 50.9 Ma \pm 5 Ma (Beamud et al.,
 2011; Fitzgerald et al., 1999; Thomson et al., 2019; Whitchurch et al., 2011). Additionally, these major changes from at least
 56 Ma onwards correspond to the main onset of flexural subsidence (Vergés et al., 1995), the regional flooding of the basin
 at the base of the Eocene (Ilerdian transgression, represented in stratigraphy by the basal *Alveolina* limestones) and the
 subsequent arrival of the main siliciclastic (i.e. Corones system in the eastern Pyrenees, Roda, Castigaleu and Castissent fluvio-
 405 deltaic systems in the central Pyrenees, Garcés et al., 2020; Puigdefàbregas and Souquet, 1986; Vergés et al., 2002), which is
 also expressed in a pronounced increase of sediment supply to the South-Pyrenean foreland basin. This period is also marked
 in the North Pyrenean domain by the activation of important coarse-grained depositional systems such as the Poudingues de
 Palassou Formation (Vacherat et al., 2017). Altogether, these observations point to a scenario in which increased convergence
 and tectonic uplift lead to topographic growth and augmentation of sediment flux, as predicted by classical landscape evolution
 410 principles (e.g., Bonnet and Crave, 2003; Whipple and Meade, 2006). If the early Eocene warming played a role in this period,
 it may have been in enhancing erosion and sediment supply out of the orogen, thereby possibly inhibiting topographic growth,
 which remains to be further tested.



After this period of growth, the subsequent topographic stability indicated by our isotopic record (coeval evolution of local and global $\delta^{18}O$) corresponds well with a period of overall constant convergence (Fig. 6C) with rates in a range of 2-3 mm/yr that lasted until the end of the Eocene.

Topographic growth resumed in the late Eocene to Oligocene (41-34 Ma), with increase of maximum elevation to values similar to the present-day (Curry et al., 2019). This was paired with increased convergence rate from 3 to 4 mm/yr at 33.9 Ma (EOT, Macchiavelli et al., 2017), which persisted until the Oligocene-Miocene boundary, and a major increase of sediment flux. Those observations, as above, are consistent with a scenario according to which tectonics drove surface uplift, increased erosion and sediment flux to peripheral basins. Contrary to the situation in the early Eocene however, the coeval shift towards colder climates that took place in the background, including the abrupt cooling at the EOT boundary, may have enhanced topographic growth by decreasing the overall erosional efficiency, and thus possibly inhibited sediment flux out of the orogen. Indeed, it is remarkable that several valleys on the southern flank of the orogen became progressively filled by continental deposits from the middle to late Eocene (Biro, 1937; Reille, 1971; Vincent, 2001; Beamud et al., 2003; Babault et al., 2005; Costa et al., 2010). In this view, cooling and aridification may have decreased the sediment transport capacity of fluvial systems draining the orogen and induced their aggradation on the wedge-top, possibly in combination with closing and continentalization of the Ebro basin from 36 Ma onwards (Costa et al., 2010). In turn, as suggested by Costa et al (2010), the aggradation of sediment in the foreland could have lowered the orogenic wedge taper, stabilizing frontal thrusts, and hence forced a renewal of exhumation of the axial zone by out-of-sequence thrusting and underplating in the inner wedge (e.g., Puigdefabregas et al., 1992; Vergès & Burbank, 1996; Sinclair et al., 2005). The fact that wedge-top sediment aggradation in the middle to late Eocene precedes the acceleration of exhumation in the Axial Zone as deduced from fission track data (e.g., from 35.0 to 32.0 Ma, Fitzgerald et al., 1999; Sinclair et al., 2005; peak exhumation at 30 Ma according to Whitchurch et al., 2011, Fig. 6) implies it does not need to be linked to increased sediment flux, but rather to interruption of sediment bypass and increasing accommodation as could possibly be due to a transition to colder climate and a decline of the transport capacity of Pyrenean fluvial systems, enhanced at 36 Ma by disconnection from the ocean basin. In this scenario, climate (decreasing erosional efficiency) could have forced topographic growth before the acceleration of Iberia-Eurasia convergence rate, and then contributed to enhance the effect of tectonically driven topographic growth that is clearly responsible of the major increase of sediment flux in the Oligocene (Fig. 6). Yet, timing is the key to cause and effect, and the timing of variations of geological parameters that we discuss here (convergence rate, exhumation, topographic growth, sediment flux), as well as their relations of subsequence or antecedence, are dependent on the resolution of the data used to infer them, among which the segmentation of geological time in discrete periods of variable duration (Ypresian, Bartonian, Priabonian, Oligocene, or magnetozone) which probably impose artificially abrupt changes of the rates presented here, and thus must be interpreted with caution.



Although beyond the scope of this paper, we also note that the documented period of topographic stability in the middle Eocene (49-41 Ma), in the general context of cooling and decreasing erosional efficiency discussed above, could also be consistent with Babault et al (2005), who proposed that continental sedimentation in the foreland paired with constant elevation of the range may have initiated a decrease of local relief within the Axial Zone of the Pyrenees as early as the middle Eocene, and not incompatible with the subsequent increase of maximum elevation in the late Eocene-Oligocene (41-34 Ma) also discussed above. This could be responsible for the origin of high-elevation, low-relief surfaces that are a subject of debate (see among others Babault et al, 2005; Ortuño and Viaplana-Muzas, 2018; and the synthesis by Calvet et al., 2020).

Eventually, convergence slowed to 0.2 mm/yr in the Miocene (Macchiavelli et al., 2017) and topography began to slowly decline (Curry et al., 2019), paired with a sharp drop in sediment flux out of the orogen. This slow topographic decline coeval with cessation of tectonics, despite the warmer climates of the Miocene compared to the Oligocene, also advocates for a weak influence of climate, or only secondary to tectonics, in the topographic evolution of the Pyrenees. perhaps also enhanced by the colder climates, which is consistent with Both observations support a stronger tectonic, rather than climatic, control on the long-term topographic evolution of the Pyrenees.

Therefore, the topographic development of the Pyrenean orogen documented here appears to be primarily determined by the dynamics of plate convergence (Eurasia and Iberia) over the Cenozoic, with climate playing an influence that remains to be demonstrated.

Response times

Considering those caveats, assuming that the timing of the acceleration of plate convergence is correct (at 56 ± 2 Ma, Machiavelli et al., 2017), and that the topography reached maximum elevation of 2000 ± 500 m at 49 Ma (this work), a first-order estimate of 7 ± 2 Ma for the response time of the Pyrenean orogen to tectonics in the early Eocene is proposed. This is similar to the duration of the late Eocene topographic growth from 41 to 34 Ma obtained by Curry et al (2019). Despite all the uncertainties mentioned above, these estimates are nevertheless in excellent agreement with classical model predictions for the response time of topography to increase in tectonic uplift in orogens (e.g., Whipple, 2001). Likewise, the resilience of high-topography after the decline of convergence such as outlined by Curry et al (2019) for the post-Oligocene evolution of the range is also consistent with the long response times predicted in situation of decreasing tectonic uplift (Whipple, 2001).

The timescales of several millions of years over which the early Eocene warming, and middle to late Eocene cooling, took place (the 30Ma-long early Cenozoic climate “hump”), are much larger than the response time of the Pyrenean orogen estimated here (with respect to tectonics) and also than the response time to climate estimated in landscape evolution models (e.g., less than several Ma, Whipple 2001; Whipple and Meade, 2006). In such conditions, where the timescale of a perturbation (here climate) is larger than the timescale of orogen response, the erosional system is predicted to remain in a constant state of



dynamic equilibrium with changing erosional efficiency (e.g., Paola et al., 1992, Whipple and Meade, 2006). This is consistent with our observation that the main periods of topographic growth and sediment flux in the Pyrenees at 54-49 Ma and 41-34 Ma are primarily forced by increased tectonic convergence and uplift over these intervals. Such estimates of response times are key elements to further knowledge about landscape response to environmental perturbations and understanding the stratigraphic record of climate and tectonics (e.g., Castelltort and Van Den Driessche, 2003, Romans et al., 2016, Tofelde et al., 2020).

This result does not challenge other findings of several studies which have documented the effect of warming events such as the PETM and other hyperthermals on enhancing erosion and transport (e.g., Schmitz and Pujalte, 2003, 2007, Foreman, 2012, Chen et al., 2018, Honegger et al., 2020) because such observations are consistent with the prediction of landscape evolution models that erosion can be reactive to high-frequency climate perturbations (e.g., Whipple, 2001, Bonnet and Crave, 2003).

Interestingly, if maximum elevation stayed at 2000 ± 500 m from 49 to 41 Ma during a period of generally continued and constant convergence, the Pyrenees could have reached a form of “steady state” topography and exhumation (e.g., Willett and Brandon, 2002) during 8 Ma in the early to middle Eocene (49-41 Ma).

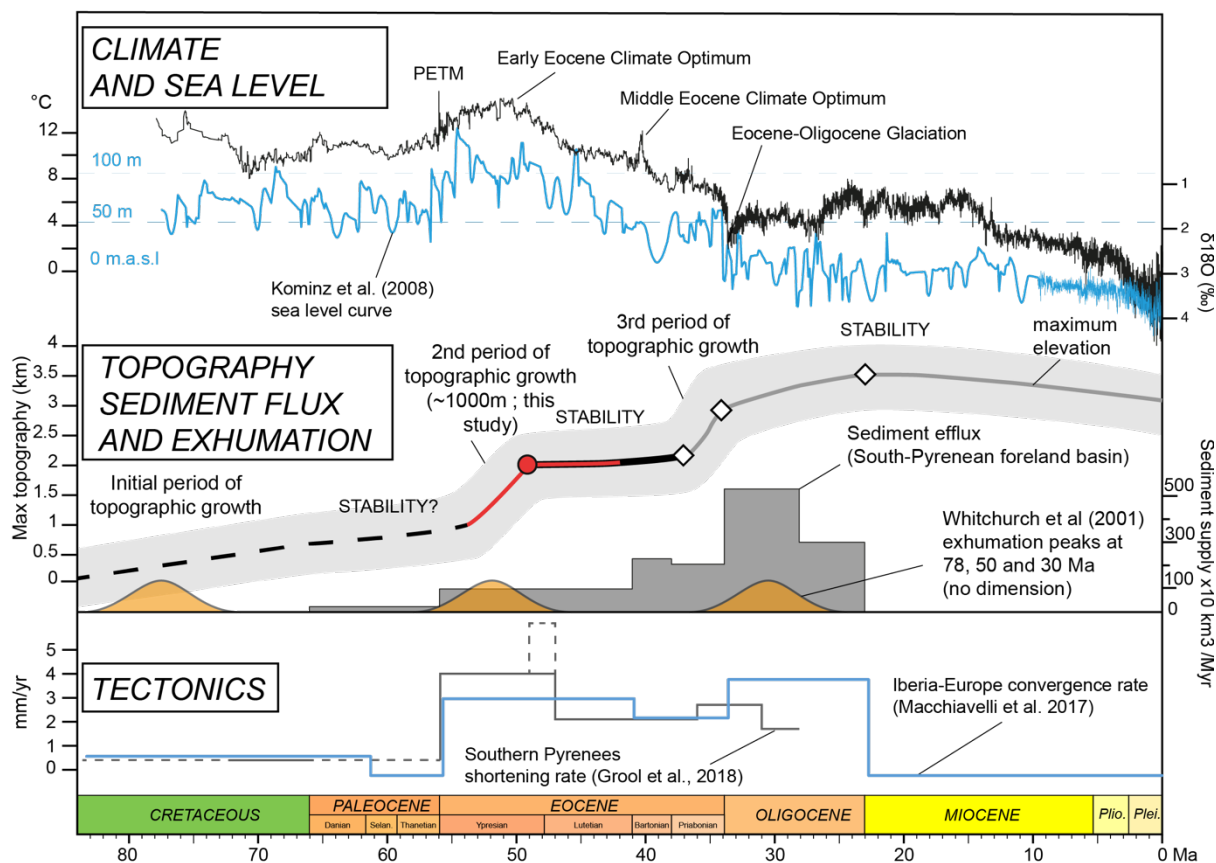




Figure 6 – Paleotopography evolution of the Pyrenees. Eocene to present maximum paleotopography modified after Curry et al. (2019) with estimates from Huyghe et al. (2012) and this study (red). The main periods of topographic growth are consistent with the peak exhumation periods from Whitchurch et al. (2011). Emerged Pyrenean mountain range timing from Vacherat et al. (2017) and end of deformation timing from Vergés et al. (2002). Dashed grey lines in shortening rates indicate high uncertainty (Grool et al., 2018). Maximum elevation here is presented with reference to Huyghe et al. (2012) and Curry et al. (2019), but our study does not carry constraints on absolute elevation values. Gray area represent the uncertainty based on Curry et al., 2019 for Lutetian to present, and on Huyghe et al., 2012, for the early Eocene.

Conclusions

Our study presents the first continuous isotopic record from marine whole-rock material from the South-Pyrenean foreland basin, and uses it to discuss the topographic evolution of the Pyrenees in the context of its tectonic evolution and of major climate variations of the Paleogene. We measured 658 samples collected on three correlated sections in the adjacent Tremp-Graus and Ainsa basins providing a novel 12 Ma-long oxygen isotope record on marine carbonates encompassing the entire early to middle Eocene succession of the South-Pyrenean foreland basin. This record allows us to significantly refine, and provide additional evidence of major topographic growth of the Pyrenees between 54 and 49 Ma to a maximum elevation of 2000 ± 500 m. Despite the important uncertainties inherent to such estimates in deep time, this result, combined with previous constraints on middle Eocene to late Oligocene topography, provides a first-order narrative of the topographic growth of the Pyrenees from its initiation to the end of convergence. This narrative, when compared with the current knowledge about the tectonic and climatic boundary conditions of the Pyrenean orogen, suggests that tectonics was the primary driver of topographic growth. Although climate may have played a role in enhancing or inhibiting topographic growth and erosion, the correlation between periods of increased convergence, increased sediment supply and increased elevation all point out to the dominant role of tectonics in driving the topographic evolution of the Pyrenees.

Our study also provides consistent estimates of 7 ± 2 Ma for the response time of the Pyrenean orogen to tectonics, a result in agreement with classical predictions of landscape evolution models. Our results highlight that the Pyrenees are an ideal natural laboratory providing a wealth of data amenable to test conceptual and analytical/numerical models of landscape evolution, especially coupling landscape evolution, tectonics of orogenic wedges and sedimentation.

Finally, these results demonstrate that $\delta^{18}\text{O}$ whole-rock data from foreland basins have the potential to faithfully record paleoenvironmental variations and can corroborate results from oceanic sites, if not altogether offer an alternative to oceanic sites, while providing tools for a better understanding of the interaction between tectonic and climatic signals in active settings.



525 Supplement link

Author contribution

LH performed the study during his PhD, including field work, sample preparation, interpretation and writing of the paper. SC designed and supervised the project and its funding, and wrote the paper. JS and TA supervised and performed the analyses and contributed to interpretation and writing. MP-M, MG, LV and DH contributed to interpretation and writing. TA, MP-M, 530 CP, MG, AV, LV, CL, AN, AF, JC and SC contributed to sampling and field work. AO provided sediment flux estimates and contributed to writing. MC contributed to interpretations and writing.

Competing interests

The authors declare that they have no conflict of interest.

Acknowledgements

535 Thanks are due to the Universities of Geneva and Lausanne for providing access to facilities and competitive rates for analyses in the frame of the Joint Geneva and Lausanne School of Earth Sciences (ELSTE). Partial financial support at different stages of this work was provided by the Department of Public Instruction of the state of Geneva, a research collaboration between Geneva and Equinor, the S2S project of the TOTAL-BRGM Orogen program, and the Swiss National Science Foundation project ESS2 (grant number 200020_182017).

540

References

- Akhil, V. P., Lengaigne, M., Durand, F., Vialard, J., Chaitanya, A. V. S., Keerthi, M. G., Gopalakrishna, V. V., Boutin, J. and de Boyer Montégut, C.: Assessment of seasonal and year-to-year surface salinity signals retrieved from SMOS and Aquarius missions in the Bay of Bengal, *Int. J. Remote Sens.*, 37(5), 1089–1114, <https://doi.org/10.1080/01431161.2016.1145362>, 2016.
- 545 Alonso, J., Pulgar, J., García-Ramos, J., Barba, P., Friend, P. and Dabrio, C.: W5 Tertiary basins and Alpine tectonics in the Cantabrian Mountains (NW Spain), *Tert. basins Spain Stratigr. Rec. crustal Kinemat.*, 214–227, 1996.
- Ambach, W., Dansgaard, W., Eisner, H. and Møller, J.: The altitude effect on the isotopic composition of precipitation and 550 glacier ice in the Alps, *Tellus*, 20(4), 595–600, <https://doi.org/10.3402/tellusa.v20i4.10040>, 1968.



- Andreasson, F. P. and Schmitz, B.: Temperature seasonality in the early middle Eocene North Atlantic region: Evidence from stable isotope profiles of marine gastropod shells, *Bull. Geol. Soc. Am.*, 112(4), 628–640, [https://doi.org/10.1130/0016-7606\(2000\)112<628:TSITEM>2.0.CO;2](https://doi.org/10.1130/0016-7606(2000)112<628:TSITEM>2.0.CO;2), 2000.
- 555
- Arche, A., Evans, G. and Clavell, E.: Some considerations on the initiation of the present SE Ebro river drainage system: Post- or pre-Messinian?, *J. Iber. Geol.*, 36(1), 73–85, <https://doi.org/10.5209/JIGE.33869>, 2010.
- Babault, J., Van Den Driessche, J., Bonnet, S., Castelltort, S. and Crave, A.: Origin of the highly elevated Pyrenean peneplain, *Tectonics*, 24(2), 1–19, <https://doi.org/10.1029/2004TC001697>, 2005.
- 560
- Beamud, E., Garcés, M., Cabrera, L., Anton Muñoz, J. and Almar, Y.: A new middle to late Eocene continental chronostratigraphy from NE Spain, *Earth Planet. Sci. Lett.*, 216(4), 501–514, [https://doi.org/10.1016/S0012-821X\(03\)00539-9](https://doi.org/10.1016/S0012-821X(03)00539-9), 2003.
- 565
- Beamud, E., Muñoz, J. A., Fitzgerald, P. G., Baldwin, S. L., Garcés, M., Cabrera, L. and Metcalf, J. R.: Magnetostratigraphy and detrital apatite fission track thermochronology in syntectonic conglomerates: Constraints on the exhumation of the South-Central Pyrenees, *Basin Res.*, 23(3), 309–331, <https://doi.org/10.1111/j.1365-2117.2010.00492.x>, 2011.
- 570
- Behar, F., Beaumont, V., Penteado, H. L. D. B. and Penteado, H. L. De B.: Rock-Eval 6 Technology: Performances and Developments, *Oil Gas Sci. Technol.*, 56(2), 111–134, <https://doi.org/10.2516/ogst:2001013>, 2001.
- Bentham, P. and Burbank, D. W.: Chronology of Eocene foreland basin evolution along the western oblique margin of the South–Central Pyrenees, in *Tertiary Basins of Spain*, edited by P. F. Friend and C. J. Dabrio, pp. 144–152, Cambridge Univ. Press, New York, <https://doi.org/10.1017/cbo9780511524851.022>, 1996.
- 575
- Biot, P.: *Recherches sur la morphologie des Pyrénées orientales franco-espagnoles*, J.-B. Baillière, 1937.
- Bonnet, S. and Crave, A.: Landscape response to climate change: Insights from experimental modeling and implications for tectonic versus climatic uplift of topography, *Geology*, 31(2), 123–126, [https://doi.org/10.1130/0091-7613\(2003\)031<0123:LRTCCI>2.0.CO;2](https://doi.org/10.1130/0091-7613(2003)031<0123:LRTCCI>2.0.CO;2), 2003.
- 580
- Brand, W. A., Coplen, T. B., Vogl, J., Rosner, M. and Prohaska, T.: Assessment of international reference materials for isotope-ratio analysis (IUPAC Technical Report), *Pure Appl. Chem.*, 86(3), 425–467, 2014.
- 585



- Calvet, M., Gunnell, Y. and Laumonier, B.: Denudation history and palaeogeography of the Pyrenees and their peripheral basins: an 84-million-year geomorphological perspective, *Earth-Science Rev.*, 103436, <https://doi.org/10.1016/j.earscirev.2020.103436>, 2020.
- 590 Campani, M., Mulch, A., Kempf, O., Schlunegger, F. and Mancktelow, N.: Miocene paleotopography of the Central Alps, *Earth Planet. Sci. Lett.*, 337–338, 174–185, <https://doi.org/10.1016/j.epsl.2012.05.017>, 2012.
- Castelltort, S., Honegger, L., Adatte, T., Clark, J. D., Puigdefàbregas, C., Spangenberg, J. E., Dykstra, M. L. and Fildani, A.: Detecting eustatic and tectonic signals with carbon isotopes in deep-marine strata, Eocene Ainsa Basin, Spanish Pyrenees, *Geology*, 45(8), 707–710, <https://doi.org/10.1130/G39068.1>, 2017.
- 595 Castelltort, S., & Van Den Driessche, J.: How plausible are high-frequency sediment supply-driven cycles in the stratigraphic record? *Sedimentary Geology*, 157(1-2), 3–13. [http://doi.org/10.1016/S0037-0738\(03\)00066-6](http://doi.org/10.1016/S0037-0738(03)00066-6), 2003
- 600 Castelltort, S., Whittaker, A. and Vergés, J.: Tectonics, sedimentation and surface processes: From the erosional engine to basin deposition, *Earth Surf. Process. Landforms*, 40(13), 1839–1846, <https://doi.org/10.1002/esp.3769>, 2015.
- Caves Rugenstein, J. K. and Chamberlain, C. P.: The evolution of hydroclimate in Asia over the Cenozoic: A stable-isotope perspective, *Earth-Science Rev.*, 185(May), 1129–1156, <https://doi.org/10.1016/j.earscirev.2018.09.003>, 2018.
- 605 Cerling, T. E.: The stable isotopic composition of modern soil carbonate and its relation to climate, *Earth Planet. Sci. Lett.*, 71, 229–240., 1984. Cerling, T. E.: The stable isotopic composition of modern soil carbonate and its relationship to climate, *Earth Planet. Sci. Lett.*, 71(2), 229–240 [papers3://publication/uuid/5E0BA588-CC89-4396-A50F-1F01574B4A12](https://doi.org/10.1016/0012-821X(84)90033-3), 1984.
- 610 Chanvry, E., Deschamps, R., Joseph, P., Puigdefàbregas, C., Poyatos-Moré, M., Serra-Kiel, J., Garcia, D. and Teinturier, S.: The influence of intrabasinal tectonics in the stratigraphic evolution of piggyback basin fills: Towards a model from the Tremp-Graus-Ainsa Basin (South-Pyrenean Zone, Spain), *Sediment. Geol.*, 377, 34–62, <https://doi.org/10.1016/j.sedgeo.2018.09.007>, 2018.
- 615 Chen, C., Guerit, L., Foreman, B. Z., Hassenruck-Gudipati, H. J., Adatte, T., Honegger, L., Perret, M., Sluijs, A. and Castelltort, S.: Estimating regional flood discharge during Palaeocene-Eocene global warming, *Sci. Rep.*, 8(1), 1–8, <https://doi.org/10.1038/s41598-018-31076-3>, 2018



- Chevrot, S., Sylvander, M., Diaz, J., Martin, R., Mouthereau, F., Manatschal, G., Masini, E., Calassou, S., Grimaud, F.,
 620 Pauchet, H. and Ruiz, M.: The non-cylindrical crustal architecture of the Pyrenees, *Sci. Rep.*, 8(1), 1–8,
<https://doi.org/10.1038/s41598-018-27889-x>, 2018.
- Choukroune, P., Daignières, M., Deramond, J., Grasso, J. R., Hirn, A., Marthelot, J. N., Mattauer, M., Seguret, M., Damotte,
 625 B., Roure, F., Cazes, M., Toreilles, G., Villien, A., Mediavila, F., Vauthier, A., Banda, E., Fontboté, J. M., Gallart, J.,
 Santanach, P., Suriñach, E., Barnolas, A., Del Valle, J., Plata, J. L., Berastagui, X., Muñoz, J. A., Puigdefabregas, C., López-
 Arroyo, A., Rivero, Arrieta, A., Camara, P., Garrido, A. and Martínez, J.: The Eors Pyrenean deep seismic profile reflection
 data and the overall structure of an orogenic belt, *Tectonics*, 8(1), 23–39, <https://doi.org/10.1029/TC008i001p00023>, 1989.
- 630 Clark, J., Puigdefabregas, C., Castelltort, S. and Fildani, A.: Propagation of Environmental Signals Within Source-to-sink
 Stratigraphy: Spanish Pyrenees, June 5th–9th, 2017, SEPM (Society for Sedimentary Geology), 2017.
- Costa, E., Garcés, M., López-Blanco, M., Beamud, E., Gómez-Paccard, M. and Larrasoña, J. C.: Closing and
 continentalization of the South Pyrenean foreland basin (NE Spain): Magnetochronological constraints, *Basin Res.*, 22(6),
 635 904–917, <https://doi.org/10.1111/j.1365-2117.2009.00452.x>, 2010.
- Cramer, B. S., Wright, J. D., Kent, D. V. and Aubry, M. P.: Orbital climate forcing of $\delta^{13}\text{C}$ excursions in the late Paleocene-
 early Eocene (chrons C24n–C25n), *Paleoceanography*, 18(4), 1–25, <https://doi.org/10.1029/2003PA000909>, 2003.
- 640 Cramer, B. S., Toggweiler, J. R., Wright, J. D., Katz, M. E. and Miller, K. G.: Ocean overturning since the Late Cretaceous:
 Inferences from a new benthic foraminiferal isotope compilation, *Paleoceanography*, 24(4), 1–14,
<https://doi.org/10.1029/2008PA001683>, 2009.
- Crochet, B.: Molasses syntectoniques du versant nord des Pyrénées: la série de Palassou, Ph.D. thesis, Université de Toulouse
 645 3, 1989
- Currie, B. S., Rowley, D. B. and Tabor, N. J.: Middle Miocene paleoaltimetry of southern Tibet: Implications for the role of
 mantle thickening and delamination in the Himalayan orogen, *Geology*, 33(3), 181–184, <https://doi.org/10.1130/G21170.1>,
 2005.
- 650



- Curry, M. E., van der Beek, P., Huisman, R. S., Wolf, S. G. and Muñoz, J. A.: Evolving paleotopography and lithospheric flexure of the Pyrenean Orogen from 3D flexural modeling and basin analysis, *Earth Planet. Sci. Lett.*, 515, 26–37, <https://doi.org/10.1016/j.epsl.2019.03.009>, 2019.
- 655 Dansgaard, W.: Stable isotopes in precipitation, *Tellus*, 16(4), 436–468, <https://doi.org/10.3402/tellusa.v16i4.8993>, 1964.
- Espitalié, J., Deroo, G. and Marquis, F.: La pyrolyse Rock-Eval et ses applications., *Rev. - Inst. Fr. du Pet.*, 40(5), 563–579, <https://doi.org/10.2516/ogst.1985045>, 1985.
- 660 Filleaudeau, P. Y., Mouthereau, F. and Pik, R.: Thermo-tectonic evolution of the south-central Pyrenees from rifting to orogeny: Insights from detrital zircon U/Pb and (U-Th)/He thermochronometry, *Basin Res.*, 24(4), 401–417, <https://doi.org/10.1111/j.1365-2117.2011.00535.x>, 2012.
- Filleaudeau, P.-Y.: Croissance et dénudation des Pyrénées du Crétacé supérieur au Paléogène: apports de l’analyse de bassin et thermochronométrie détritique, Ph.D. thesis, Université Pierre et Marie Curie-Paris VI, 2011.
- 665 et thermochronométrie détritique, Ph.D. thesis, Université Pierre et Marie Curie-Paris VI, 2011.
- Fillon, C. and van der Beek, P.: Post-orogenic evolution of the southern Pyrenees: Constraints from inverse thermo-kinematic modelling of low-temperature thermochronology data, *Basin Res.*, 24(4), 418–436, <https://doi.org/10.1111/j.1365-2117.2011.00533.x>, 2012.
- 670 Fitzgerald, P. G., Muñoz, J. A., Coney, P. J. and Baldwin, S. L.: Asymmetric exhumation across the Pyrenean orogen: Implications for the tectonic evolution of a collisional orogen, *Earth Planet. Sci. Lett.*, 173(3), 157–170, [https://doi.org/10.1016/S0012-821X\(99\)00225-3](https://doi.org/10.1016/S0012-821X(99)00225-3), 1999.
- 675 Ford, M., Hemmer, L., Vacherat, A., Gallagher, K. and Christophoul, F.: Retro-wedge foreland basin evolution along the ECORS line, eastern Pyrenees, France, *J. Geol. Soc. London.*, 173(3), 419–437, 2016.
- Foreman, B. Z., Heller, P. L. and Clementz, M. T.: Fluvial response to abrupt global warming at the Palaeocene/Eocene boundary, *Nature*, 491(7422), 92–95, <https://doi.org/10.1038/nature11513>, 2012.
- 680 France-Lanord, C., Derry, L. and Michard, A.: Evolution of the Himalaya since Miocene time: Isotopic and sedimentological evidence from the Bengal Fan, *Geol. Soc. Spec. Publ.*, 74, 603–621, <https://doi.org/10.1144/GSL.SP.1993.074.01.40>, 1993.



- 685 Fricke, H. C.: Investigation of early Eocene water-vapor transport and paleoelevation using oxygen isotope data from
 geographically widespread mammal remains, *Bull. Geol. Soc. Am.*, 115(9), 1088–1096, <https://doi.org/10.1130/B25249.1>,
 2003.
- Garcés, M., López-Blanco, M., Valero, L., Beamud, E., Muñoz, J. A., Oliva-Urcia, B., Vinyoles, A., Arbués, P., Cabello, P.
 and Cabrera, L.: Paleogeographic and sedimentary evolution of the south-pyrenean foreland basin, *Mar. Pet. Geol.*, 113(May
 690 2019), 104105, <https://doi.org/10.1016/j.marpetgeo.2019.104105>, 2020.
- Garcia-Castellanos, D., Vergés, J., Gaspar-Escribano, J. and Cloetingh, S.: Interplay between tectonics, climate, and fluvial
 transport during the Cenozoic evolution of the Ebro Basin (NE Iberia), *J. Geophys. Res. Solid Earth*, 108(B7),
<https://doi.org/10.1029/2002jb002073>, 2003.
- 695 Garzione, C. N., Dettman, D. L., Quade, J., De Celles, P. G. and Butler, R. F.: High times on the Tibetan Plateau: Paleoelevation
 of the Thakkhola graben, Nepal, *Geology*, 28(4), 339–342, [https://doi.org/10.1130/0091-7613\(2000\)28<339:HTOTTP>2.0.CO;2](https://doi.org/10.1130/0091-7613(2000)28<339:HTOTTP>2.0.CO;2), 2000.
- 700 Garzione, C. N., Dettman, D. L. and Horton, B. K.: Carbonate oxygen isotope paleoaltimetry: evaluating the effect of
 diagenesis on paleoelevation estimates for the Tibetan plateau, *Palaeogeogr. Palaeoclimatol. Palaeoecol.*, 212(1–2), 119–140,
<https://doi.org/10.1016/j.palaeo.2004.05.020>, 2004.
- Garzione, C. N., Molnar, P., Libarkin, J. C. and MacFadden, B. J.: Rapid late Miocene rise of the Bolivian Altiplano: Evidence
 705 for removal of mantle lithosphere, *Earth Planet. Sci. Lett.*, 241(3–4), 543–556, <https://doi.org/10.1016/j.epsl.2005.11.026>,
 2006.
- Gómez-Gras, D., Roigé, M., Fondevilla, V., Oms, O., Boya, S. and Remacha, E.: Provenance constraints on the Tremp
 Formation paleogeography (southern Pyrenees): Ebro Massif VS Pyrenees sources, *Cretac. Res.*, 57, 414–427,
 710 <https://doi.org/10.1016/j.cretres.2015.09.010>, 2016.
- Grool, A. R., Ford, M., Vergés, J., Huisman, R. S., Christophoul, F. and Dielforder, A.: Insights Into the Crustal-Scale
 Dynamics of a Doubly Vergent Orogen From a Quantitative Analysis of Its Forelands: A Case Study of the Eastern Pyrenees,
Tectonics, 37(2), 450–476, <https://doi.org/10.1002/2017TC004731>, 2018.



- Gunnell, Y., Zeyen, H. and Calvet, M.: Geophysical evidence of a missing lithospheric root beneath the Eastern Pyrenees: Consequences for post-orogenic uplift and associated geomorphic signatures, *Earth Planet. Sci. Lett.*, 276(3–4), 302–313, <https://doi.org/10.1016/j.epsl.2008.09.031>, 2008.
- 720 Haseldonckx, P.: The palynology of some Palaeogene deposits between the Rio Esera and the Rio Segre, southern Pyrenees, Spain, *Leidse Geol. Meded.*, 49(1), 145–165, 1973.
- Heard, T. G., Pickering, K. T. and Robinson, S. A.: Milankovitch forcing of bioturbation intensity in deep-marine thin-bedded siliciclastic turbidites, *Earth Planet. Sci. Lett.*, 272(1–2), 130–138, <https://doi.org/10.1016/j.epsl.2008.04.025>, 2008.
- 725 Hewitt, G.: The genetic legacy of the quaternary ice ages, *Nature*, 405(6789), 907–913, <https://doi.org/10.1038/35016000>, 2000.
- Honegger, L., Adate, T., Spangenberg, J. E., Caves Rugenstein, J. K., Poyatos-Moré, M., Puigdefàbregas, C., Chanvry, E.,
 730 Clark, J., Fildani, A., Verrechia, E., Kouzmanov, K., Harlaux, M. and Castelltort, S.: Alluvial record of an early Eocene hyperthermal within the Castissent Formation, the Pyrenees, Spain, *Clim. Past*, 16(1), 227–243, <https://doi.org/10.5194/cp-16-227-2020>, 2020.
- Huyghe, D., Castelltort, S., Mouthereau, F., Serra-Kiel, J., Filleaudeau, P. Y., Emmanuel, L., Berthier, B. and Renard, M.:
 735 Large scale facies change in the middle Eocene South-Pyrenean foreland basin: The role of tectonics and prelude to Cenozoic ice-ages, *Sediment. Geol.*, 253–254, 25–46, <https://doi.org/10.1016/j.sedgeo.2012.01.004>, 2012.
- Huyghe, D., Mouthereau, F., Ségalen, L. and Furió, M.: Long-term dynamic topographic support during post-orogenic crustal thinning revealed by stable isotope ($\delta^{18}\text{O}$) paleo-altimetry in eastern Pyrenees, *Sci. Rep.*, 10(1), 1–8,
 740 <https://doi.org/10.1038/s41598-020-58903-w>, 2020.
- Jenkyns, H. C.: Relative sea-level change and carbon isotopes: Data from the Upper Jurassic (Oxfordian) of central and Southern Europe, *Terra Nov.*, 8, 75–85, 1996. Jenkyns, H. C.: Relative sea-level change and carbon isotopes: Data from the Upper Jurassic (Oxfordian) of central and Southern Europe, *Terra Nov.*, 8(1), 75–85, <https://doi.org/10.1111/j.1365-3121.1996.tb00727.x>, 1996.
- 745 Kominz, M. A., Browning, J. V., Miller, K. G., Sugarman, P. J., Mizintseva, S. and Scotese, C. R.: Late Cretaceous to Miocene sea-level estimates from the New Jersey and Delaware coastal plain coreholes: An error analysis, *Basin Res.*, 20(2), 211–226, <https://doi.org/10.1111/j.1365-2117.2008.00354.x>, 2008.



750

Kroopnick, P. M.: The distribution of ^{13}C of ΣCO_2 in the world oceans, *Deep Sea Res. Part A, Oceanogr. Res. Pap.*, 32(1), 57–84, [https://doi.org/10.1016/0198-0149\(85\)90017-2](https://doi.org/10.1016/0198-0149(85)90017-2), 1985.

Kukla, T., Winnick, M. J., Maher, K., Ibarra, D. E. and Chamberlain, C. P.: The Sensitivity of Terrestrial $\delta^{18}\text{O}$ Gradients to
 755 Hydroclimate Evolution, *J. Geophys. Res. Atmos.*, 124(2), 563–582, <https://doi.org/10.1029/2018JD029571>, 2019.

Läuchli, C., Garcés, M., Beamud, B., Valero, L., Honegger, L., Adatte, T., Spangenberg, J. E., Clark, J., Puigdefabregas, C.,
 Fildani, A., de Kaenel, E., Hunger, T., Nowak, A. and Castelltort, S.: Magnetostratigraphy and stable isotope stratigraphy of
 the middle-Eocene succession of the Ainsa basin (Spain): new age constraints and implications for sediment delivery to the
 760 deep waters, submitted to *Mar. Pet. Geol.*, preprint at EarthArXiv, 2021.

Le Vine, D. M., Lagerloef, G. S. E., Colomb, F. R., Yueh, S. H. and Pellerano, F. A.: Aquarius: An instrument to monitor sea
 surface salinity from space, *IEEE Trans. Geosci. Remote Sens.*, 45(7), 2040–2050,
<https://doi.org/10.1109/TGRS.2007.898092>, 2007.

765

López-Blanco, M., Marzo, M. and Munoz, J. A.: Low-amplitude, synsedimentary folding of a deltaic complex: Roda
 Sandstone (lower Eocene), South-Pyrenean Foreland Basin, *Basin Res.*, 15(1), 73–96, <https://doi.org/10.1046/j.1365-2117.2003.00193.x>, 2003.

770 Raymo, M. E. and Ruddiman, W. F.: Tectonic Forcing of Late Cenozoic Climate, *Nature*, 117–122, 1992.

Macchiavelli, C., Vergés, J., Schettino, A., Fernández, M., Turco, E., Casciello, E., Torne, M., Pierantoni, P. P. and Tunini,
 L.: A New Southern North Atlantic Isochron Map: Insights Into the Drift of the Iberian Plate Since the Late Cretaceous, *J.*
Geophys. Res. Solid Earth, 122(12), 9603–9626, <https://doi.org/10.1002/2017JB014769>, 2017.

775

Machel, H. G., Krouse, H. R. and Sassen, R.: Products and distinguishing criteria of bacterial and thermochemical sulfate
 reduction, *Appl. Geochemistry*, 10(4), 373–389, [https://doi.org/10.1016/0883-2927\(95\)00008-8](https://doi.org/10.1016/0883-2927(95)00008-8), 1995.

Maclachlan, S. E., Cottier, F. R., Austin, W. E. N. and Howe, J. A.: The salinity: $\delta^{18}\text{O}$ water relationship in Kongsfjorden,
 780 western Spitsbergen, *Polar Res.*, 26(2), 160–167, <https://doi.org/10.1111/j.1751-8369.2007.00016.x>, 2007.



- Marshall, J. D.: Climatic and oceanographic isotopic signals from the carbonate rock record and their preservation, *Geol. Mag.*, 129(2), 143–160, <https://doi.org/10.1017/S0016756800008244>, 1992. Marshall, J.: Climatic and oceanographic isotopic signals from the carbonate rock record and their preservation, *Geol. Mag.*, 129, 143–160, 1992.
- 785 Metcalf, J. R., Fitzgerald, P. G., Baldwin, S. L. and Muñoz, J. A.: Thermochronology of a convergent orogen: Constraints on the timing of thrust faulting and subsequent exhumation of the Maladeta Pluton in the Central Pyrenean Axial Zone, *Earth Planet. Sci. Lett.*, 287(3–4), 488–503, <https://doi.org/10.1016/j.epsl.2009.08.036>, 2009.
- 790 Millán, H., Bezemer, T. Den, Vergés, J., Marzo, M., Muñoz, J. A., Roca, E., Cirés, J., Zoetemeijer, R., Cloetingh, S. and Puigdefabregas, C.: Palaeo-elevation and effective elastic thickness evolution at mountain ranges: inferences from flexural modelling in the Eastern Pyrenees and Ebro Basin, *Mar. Pet. Geol.*, 12(8), 917–928, [https://doi.org/10.1016/0264-8172\(95\)98855-Y](https://doi.org/10.1016/0264-8172(95)98855-Y), 1995.
- 795 Miller, K. G., Wright, J. D. and Fairbanks, R. G.: Unlocking the ice house: Oligocene-Miocene oxygen isotopes, eustasy, and margin erosion, *J. Geophys. Res.*, 96(B4), 6829–6848, <https://doi.org/10.1029/90JB02015>, 1991.
- Molina, E., Angori, E., Arenillas, I., Brinkhuis, H., Crouch, E. M., Luterbacher, H., Monechi, S. and Schmitz, B.: Correlation de la limite Paleocene/Eocene et l'Ilerdien dans la coupe de Campo, Espagne, *Rev. Micropaleontol.*, 2(46), 95–109, 2003.
- 800 Morris, R. G., Sinclair, H. D. and Yelland, A. J.: Exhumation of the Pyrenean Orogen: implications for sediment discharge, *Basin Res.*, 10(1), 69–85, <https://doi.org/10.1046/j.1365-2117.1998.00053.x>, 1998.
- Mouthereau, F., Filleaudeau, P. Y., Vacherat, A., Pik, R., Lacombe, O., Fellin, M. G., Castelltort, S., Christophoul, F. and
 805 Masini, E.: Placing limits to shortening evolution in the Pyrenees: Role of margin architecture and implications for the Iberia/Europe convergence, *Tectonics*, 33(12), 2283–2314, <https://doi.org/10.1002/2014TC003663>, 2014.
- Mulch, A.: Stable isotope paleoaltimetry and the evolution of landscapes and life, *Earth Planet. Sci. Lett.*, 433, 180–191, <https://doi.org/10.1016/j.epsl.2015.10.034>, 2016. Mulch, A.: Stable isotope paleoaltimetry and the evolution of landscapes and
 810 life, *Earth Planet. Sci. Lett.*, 433, 180–191, <https://doi.org/10.1016/j.epsl.2015.10.034>, 2016.
- Muñoz, J. A.: Evolution of a continental collision belt: ECORS-Pyrenees crustal balanced cross-section, in *Thrust Tectonics*, pp. 235–246, Springer, Dordrecht, https://doi.org/10.1007/978-94-011-3066-0_21, 1992.



- 815 Mutti, E.: Distinctive thin-bedded turbidite facies and related depositional environments in the Eocene Hecho Group (South-central Pyrenees, Spain), *Sedimentology*, 24(1), 107–131, <https://doi.org/10.1111/j.1365-3091.1977.tb00122.x>, 1977.
- Mutti, E., Séguret, M. and Sgavetti, M.: Sedimentation and deformation in the Tertiary Sequences of the Southern Pyrenees: Field trip 7, AAPG Mediterr. basins Conf., 7, 1988.
- 820 Nijman, W.: Cyclicity and basin axis shift in a piggyback basin: towards modelling of the Eocene Tremp-Ager Basin, South Pyrenees, Spain, *Geol. Soc. London, Spec. Publ.*, 134(1), 135–162, <https://doi.org/10.1144/GSL.SP.1998.134.01.07>, 1998.
- Odum, M. L., Stockli, D. F., Capaldi, T. N., Thomson, K. D., Clark, J., Puigdefàbregas, C. and Fildani, A.: Tectonic and
 825 sediment provenance evolution of the South Eastern Pyrenean foreland basins during rift margin inversion and orogenic uplift, *Tectonophysics*, 765(February), 226–248, <https://doi.org/10.1016/j.tecto.2019.05.008>, 2019.
- Ortiz, A., Guillocheau, F., Lasseur, E., Briaies, J., Robin, C., Serrano, O. and Fillon, C.: Sediment routing system and sink
 830 Bay of Biscay) Basins, *Mar. Pet. Geol.*, 112, 104085, <https://doi.org/10.1016/j.marpetgeo.2019.104085>, 2020.
- Ortuño, M., Martí, A., Martín-Closas, C., Jiménez-Moreno, G., Martinetto, E. and Santanach, P.: Palaeoenvironments of the late miocene prüedo basin: Implications for the uplift of the central pyrenees, *J. Geol. Soc. London.*, 170(1), 79–92, <https://doi.org/10.1144/jgs2011-121>, 2013.
- 835 Ortuño, M. and Viaplana-Muzas, M.: Active fault control in the distribution of elevated low relief topography in the central-western pyrenees, *Geol. Acta*, 16(4), 499–518, <https://doi.org/10.1344/GeologicaActa2018.16.4.10>, 2018.
- Page Chamberlain, C. and Poage, M. A.: Reconstructing the paleotopography of mountain belts from the isotopic composition
 840 of authigenic minerals, *Geology*, 28(2), 115–118, [https://doi.org/10.1130/0091-7613\(2000\)28<115:RTPOMB>2.0.CO](https://doi.org/10.1130/0091-7613(2000)28<115:RTPOMB>2.0.CO), 2000.
- Paillard, D., Labeyrie, L. and Yiou, P.: Macintosh program performs time-series analysis, *Eos, Trans. Am. Geophys. Union*, 77(39), 379, 1996. Paola, C., Heller, P. L. and Angevine, C. L.: The large-scale dynamics of grain-size variation in alluvial basins, 1: Theory, *Basin Res.*, 4(2), 73–90, 1992.
- 845 Payros, A., Ortiz, S., Millán, I., Arostegi, J., Orue-Etxebarria, X. and Apellaniz, E.: Early Eocene climatic optimum: Environmental impact on the North Iberian continental margin, *Bull. Geol. Soc. Am.*, 127(11–12), 1632–1644, <https://doi.org/10.1130/B31278.1>, 2015.



850 Pearson, P. N.: Oxygen Isotopes in Foraminifera: Overview and Historical Review, in *Reconstructing Earth's Deep-Time Climate—The State of the Art in 2012*, vol. 18, edited by L. C. Ivany and B. T. Huber, pp. 1–38, The Paleontological Society Papers, <https://doi.org/10.1017/s1089332600002539>, , 2012.

855 Pickering, K. T. and Corregidor, J.: Mass-transport complexes (MTCs) and tectonic control on basin-floor submarine fans, middle Eocene, South Spanish Pyrenees, *J. Sediment. Res.*, 75(5), 761–783, <https://doi.org/10.2110/jsr.2005.062>, 2005.

Poage, M. A. and Chamberlain, C. P.: Empirical relationships between elevation and the stable isotope composition of precipitation and surface waters: Considerations for studies of paleoelevation change, *Am. J. Sci.*, 301(1), 1–15, <https://doi.org/10.2475/ajs.301.1.1>, 2001.

860

Puigdefàbregas, C., Muñoz, J. A. and Vergés, J.: Thrusting and foreland basin evolution in the Southern Pyrenees, *Thrust Tectonics*, 247–254, https://doi.org/10.1007/978-94-011-3066-0_22, 1992.

865 Puigdefàbregas, C., Muñoz, J. J. and Vergés, J.: Thrusting and foreland basin evolution in the southern Pyrenees, *Thrust tectonics*, 247–254, 1992. Puigdefàbregas, C. and Souquet, P.: Tecto-sedimentary cycles and depositional sequences of the Mesozoic and Tertiary from the Pyrenees, *Tectonophysics*, 129(1–4), 173–203, [https://doi.org/10.1016/0040-1951\(86\)90251-9](https://doi.org/10.1016/0040-1951(86)90251-9), 1986.

870 Reille, J.-L.: Les relations entre tectorogénèse et sédimentation sur le versant sud des Pyrénées centrales: d'après l'étude de formations tertiaires essentiellement continentales, Ph.D. thesis, Univ. des Sci. et Technol. du Languedoc, Montpellier, France, 1971.

Romans, B. W., Castellort, S., Covault, J. A., Fildani, A. and Walsh, J. P.: Environmental signal propagation in sedimentary systems across timescales, *Earth-Science Rev.*, 153, 7–29, <https://doi.org/10.1016/j.earscirev.2015.07.012>, 2016.

875

Rosenbaum, G., Lister, G. S. and Duboz, C.: Relative motions of Africa, Iberia and Europe during Alpine orogeny, *Tectonophysics*, 359, 117–129, 2002.

880 Rowley, D. B. and Garzione, C. N.: Stable isotope-based paleoaltimetry, *Annu. Rev. Earth Planet. Sci.*, 35, 463–508, <https://doi.org/10.1146/annurev.earth.35.031306.140155>, 2007.



- Rowley, D. B., Pierrehumbert, R. T. and Currie, B. S.: A new approach to stable isotope-based paleoaltimetry: Implications for paleoaltimetry and paleohypsometry of the High Himalaya since the late Miocene, *Earth Planet. Sci. Lett.*, 188(1–2), 253–268, [https://doi.org/10.1016/S0012-821X\(01\)00324-7](https://doi.org/10.1016/S0012-821X(01)00324-7), 2001.
- 885
- Saltzman, M. R. and Thomas, E.: Carbon isotope stratigraphy, in *The Geologic Time Scale 2012*, pp. 207–232, Elsevier, <https://doi.org/10.1016/B978-0-444-59425-9.00011-1>, , 2012.
- Schmitz, B., Pujalte, V. and Núñez-Betelu, K.: Climate and sea-level perturbations during the Initial Eocene Thermal
 890 Maximum: Evidence from siliciclastic units in the Basque basin (Ermua, Zumaia and Trabakua Pass), northern Spain, *Palaeogeogr. Palaeoclimatol. Palaeoecol.*, 165(3–4), 299–320, [https://doi.org/10.1016/S0031-0182\(00\)00167-X](https://doi.org/10.1016/S0031-0182(00)00167-X), 2001.
- Schmitz, B. and Pujalte, V.: Sea-level, humidity, and land-erosion records across the initial Eocene thermal maximum from a continental-marine transect in northern Spain, *Geology*, 31(8), 689–692, <https://doi.org/10.1130/G19527.1>, 2003.
- 895
- Schmitz, B. and Pujalte, V.: Abrupt increase in seasonal extreme precipitation at the Paleocene-Eocene boundary, *Geology*, 35(3), 215–218, <https://doi.org/10.1130/G23261A.1>, 2007.
- Scotchman, J. I., Bown, P., Pickering, K. T., BouDagher-Fadel, M., Bayliss, N. J. and Robinson, S. A.: A new age model for
 900 the middle Eocene deep-marine Ainsa Basin, Spanish Pyrenees, *Earth-Science Rev.*, 144, 10–22, <https://doi.org/10.1016/j.earscirev.2014.11.006>, 2015.
- Séguret, M.: Étude tectonique des nappes et séries décollées de la partie centrale du versant sud des Pyrénées, *Pub. Estela, Ser geol. struct.*, 2, 1–155, 1972.
- 905
- Sheldon, N. D., Retallack, G. J. and Tanaka, S.: Geochemical climofunctions from North American soils and application to paleosols across the Eocene-Oligocene boundary in Oregon, *J. Geol.*, 110(6), 687–696, <https://doi.org/10.1086/342865>, 2002.
- Siegenthaler, U. and Oeschger, H.: Correlation of $\delta^{18}O$ in precipitation with temperature and altitude, *Nature*, 285, 314–317,
 910 1980. Siegenthaler, U. and Oeschger, H.: Correlation of $\delta^{18}O$ in precipitation with temperature and altitude, *Nature*, 285(5763), 314–317, <https://doi.org/10.1038/285314a0>, 1980.
- Sinclair, H. D., Gibson, M., Naylor, M. and Morris, R. G.: Asymmetric growth of the Pyrenees revealed through measurement and modeling of orogenic fluxes, *Am. J. Sci.*, 305(5), 369–406, <https://doi.org/10.2475/ajs.305.5.369>, 2005.
- 915



- Sømme, T. O., Helland-hansen, W., Martinsen, O. J. and Thurmond, J. B.: Relationships between morphological and sedimentological parameters in source-to-sink systems: A basis for predicting semi-quantitative characteristics in subsurface systems, *Basin Res.*, 21(4), 361–387, <https://doi.org/10.1111/j.1365-2117.2009.00397.x>, 2009.
- 920 Suc, J. P. and Fauquette, S.: The use of pollen floras as a tool to estimate palaeoaltitude of mountains: The eastern Pyrenees in the Late Neogene, a case study, *Palaeogeogr. Palaeoclimatol. Palaeoecol.*, 321–322, 41–54, <https://doi.org/10.1016/j.palaeo.2012.01.014>, 2012.
- Ternois, S., Odlum, M., Ford, M., Pik, R., Stockli, D., Tibari, B., Vacherat, A. and Bernard, V.: Thermochronological Evidence
 925 of Early Orogenesis, Eastern Pyrenees, France, *Tectonics*, 38(4), 1308–1336, <https://doi.org/10.1029/2018TC005254>, 2019.
- Thomson, K. D., Stockli, D. F., Clark, J. D., Puigdefàbregas, C. and Fildani, A.: Detrital zircon (U-Th)/(He-Pb) double-dating constraints on provenance and foreland basin evolution of the Ainsa Basin, south-central Pyrenees, Spain, *Tectonics*, 36(7), 1352–1375, <https://doi.org/10.1002/2017TC004504>, 2017.
- 930 Thomson, K. D., Stockli, D. F., Odlum, M. L., Tolentino, P., Puigdefàbregas, C., Clark, J. and Fildani, A.: Sediment provenance and routing evolution in the Late Cretaceous–Eocene Ager Basin, south-central Pyrenees, Spain, *Basin Res.*, 32(3), 485–504, <https://doi.org/10.1111/bre.12376>, 2020.
- 935 Tofelde, S., Bernhardt, A., Romans, B., & Guerit, L.: Times associated with source-to-sink propagation of environmental signals during landscape transience. *EarthArXiv* (preprint) <http://doi.org/10.31223/X5X88K>, 2020.
- Tosal, A., Verduzco, O. and Martín-Closas, C.: CLAMP-based palaeoclimatic analysis of the late Miocene (Tortonian) flora from La Cerdanya Basin of Catalonia, Spain, and an estimation of the palaeoaltitude of the eastern Pyrenees, *Palaeogeogr. Palaeoclimatol. Palaeoecol.*, 564(August 2020), 110186, <https://doi.org/10.1016/j.palaeo.2020.110186>, 2021.
- 940 Tucker, G. E. and Slingerland, R.: Drainage basin responses to climate change, *Water Resour. Res.*, 33(8), 2031–2047, <https://doi.org/10.1029/97WR00409>, 1997.
- Vacherat, A., Mouthereau, F., Pik, R., Huyghe, D., Paquette, J. L., Christophoul, F., Loget, N. and Tibari, B.: Rift-to-collision sediment routing in the Pyrenees: A synthesis from sedimentological, geochronological and kinematic constraints, *Earth-Science Rev.*, 172, 43–74, <https://doi.org/10.1016/j.earscirev.2017.07.004>, 2017.



- Vergés, J., Millán, H., Roca, E., Muñoz, J. A., Marzo, M., Cirés, J., Bezemer, T. Den, Zoetemeijer, R. and Cloetingh, S.:
 950 Eastern Pyrenees and related foreland basins: pre-, syn- and post-collisional crustal-scale cross-sections, *Mar. Pet. Geol.*, 12(8),
 903–915, [https://doi.org/10.1016/0264-8172\(95\)98854-X](https://doi.org/10.1016/0264-8172(95)98854-X), 1995.
- Vergés, J. and Burbank, D. W.: Eocene-Oligocene thrusting and basin configuration in the eastern and central Pyrenees (Spain),
 in *Tertiary Basins of Spain. World and Regional Geology*, edited by P. F. Friend and C. J. Dabrio, pp. 120–133, Cambridge
 955 University Press, 1996.
- Vergés, J., Fernández, M. and Martínez, A.: The Pyrenean orogen: Pre-, syn-, and post-collisional evolution, *J. Virtual Explor.*,
 8, 55–74, <https://doi.org/10.3809/jvirtex.2002.00058>, 2002.
- 960 Vergés, J., Millán, H., Roca, E., Muñoz, J. A., Marzo, M., Cites, J., Bezemer, T. Den, Zoetemeijer, R. and Cloetingh, S.:
 Evolution of a collisional orogen: Eastern Pyrenees transect and petroleum potential, *Ma*, 12(8), 893–915, 1995.
- Vincent, S. J.: The Sis palaeovalley: A record of proximal fluvial sedimentation and drainage basin development in response
 to Pyrenean mountain building, *Sedimentology*, 48(6), 1235–1276, <https://doi.org/10.1046/j.1365-3091.2001.00421.x>, 2001.
 965
- Watts, A. B. and Torné, M.: Crustal structure and the mechanical properties of extended continental lithosphere in the Valencia
 trough (western Mediterranean), *J. Geol. Soc. London.*, 149(5), 813–827, 1992.
- Westerhold, T., Röhl, U., Donner, B. and Zachos, J. C.: Global Extent of Early Eocene Hyperthermal Events: A New Pacific
 970 Benthic Foraminiferal Isotope Record From Shatsky Rise (ODP Site 1209), *Paleoceanogr. Paleoclimatology*, 33(6), 626–642,
<https://doi.org/10.1029/2017PA003306>, 2018.
- Whipple, K. X.: Fluvial landscape response time: How plausible is steady-state denudation?, *Am. J. Sci.*, 301(4–5), 313–325,
<https://doi.org/10.2475/ajs.301.4-5.313>, 2001.
 975
- Whipple, K. X. and Meade, B. J.: Orogen response to changes in climatic and tectonic forcing, *Earth Planet. Sci. Lett.*, 243(1–
 2), 218–228, <https://doi.org/10.1016/j.epsl.2005.12.022>, 2006.
- Whitchurch, A. L., Carter, A., Sinclair, H. D., Duller, R. A., Whittaker, A. C. and Allen, P. A.: Sediment routing system
 980 evolution within a diachronously uplifting orogen: Insights from detrital zircon thermochronological analyses from the South-
 Central pyrenees, *Am. J. Sci.*, 311(5), 442–482, <https://doi.org/10.2475/05.2011.03>, 2011.



985

Willett, S. D. and Brandon, M. T.: On steady states in mountain belts, *Geology*, 30(2), 175–178, [https://doi.org/10.1130/0091-7613\(2002\)030<0175:OSSIMB>2.0.CO;2](https://doi.org/10.1130/0091-7613(2002)030<0175:OSSIMB>2.0.CO;2), 2002.

Zachos, J., Dickens, G. and Zeebe, R.: An early Cenozoic perspective on greenhouse warming and carbon-cycle dynamics., *Nature*, 451(7176), 279–83, <https://doi.org/10.1038/nature06588>, 2008.

990

Zachos, J., Pagani, H., Sloan, L., Thomas, E. and Billups, K.: Trends, rhythms, and aberrations in global climate 65 Ma to present, *Science*, 292(5517), 686–693, <https://doi.org/10.1126/science.1059412>, 2001.

995

Zamarreño, I., Anadón, P. and Utrilla, R.: Sedimentology and isotopic composition of Upper Palaeocene to Eocene non-marine stromatolites, eastern Ebro Basin, NE Spain, *Sedimentology*, 44(1), 159–176, <https://doi.org/10.1111/j.1365-3091.1997.tb00430.x>, 1997.